United States
Environmental Protection
Agency

EPA-600/R-04-107
August 2004

Identification of (and Responses to) Potential Effects of SCR and Wet Scrubbers on Submicron Particulate Emissions and Plume Characteristics

EPA-600/R-04/107
August 2004

Identification of (and Responses to) Potential Effects of SCR and Wet Scrubbers on Submicron Particulate Emissions and Plume Characteristics

by

William E. Farthing, Peter M. Walsh, John P. Gooch
Joseph D. McCain, W. Scott Hinton, Robert F. Heaphy
Southern Research Institute
2000 Ninth Avenue South
Birmingham, Alabama 35205

Inter-Agency Agreement DW 64959501

EPA Project Officer: C. Andrew Miller
Office of Research and Development
National Risk Management Research Laboratory
Air Pollution Prevention and Control Division

Air Pollution Prevention and Control Division
National Risk Management Research Laboratory
Office of Research and Development
U. S. Environmental Protection Agency
Research Triangle Park, NC 27711

Abstract

The addition of selective catalytic reduction (SCR) systems and wet flue gas desulfurization (FGD) scrubbers to coal-fired boilers has led to substantial reductions in emissions of nitrogen oxides (NO_X) and sulfur dioxide (SO_2). However, observations of pilot- and full-scale tests of these technologies reveal potential adverse side effects that may produce operational and particulate emissions problems. The indirect effects of SCR technology of immediate interest center around its catalytic enhancement of SO_2 oxidation to sulfur trioxide (SO_3) and subsequent increases of sulfuric acid aerosols, which can produce visible near-stack plumes and acid aerosol mists. This report summarizes the current state-of-the-science concerning SO_3 formation processes and methods to minimize such formation. Corrosion of plant components such as air preheaters and other balance of plant problems are discussed, as are problems associated with operation of air pollution control equipment. Also discussed are the limitations of SO_3 measurement methods and the resulting uncertainties in many existing SO_3 emissions data. Size distributions and visible plume formation are discussed, including empirical predictions of conditions—such as coal type, sulfur content, and presence of pollution control equipment—that may lead to greater potential for visible plume formation.

Four general approaches provide a high probability for successful SO_3 removal: (1) alkali injection into the furnace, (2) humidification at the electrostatic precipitator (ESP) inlet to reduce the temperature to below the acid dew point, (3) alkali injection combined with humidification at the ESP inlet, and (4) separate wet particulate control device such as a wet ESP. All of these approaches have been tested in demonstration scale, but all must be considered new technology that will require adjustments or identifications of procedures to deal with specific sites. The first three have balance of plant issues associated with them; that is, increase risks of unforeseen negative effects on plant operation. Other concepts of interest, but less fully tested, include (1) alkali injection in duct leading to a wet FGD scrubber and (2) an electrostatically augmented mist eliminator. Various devices are being offered which have the purpose of contacting sorbents with flue gas for removal of SO_3 as well as other gaseous pollutants.

Foreword

The U.S. Environmental Protection Agency (EPA) is charged by Congress with protecting the Nation's land, air, and water resources. Under a mandate of national environmental laws, the Agency strives to formulate and implement actions leading to a compatible balance between human activities and the ability of natural systems to support and nurture life. To meet this mandate, EPA's research program is providing data and technical support for solving environmental problems today and building a science knowledge base necessary to manage our ecological resources wisely, understand how pollutants affect our health, and prevent or reduce environmental risks in the future.

The National Risk Management Research Laboratory (NRMRL) is the Agency's center for investigation of technological and management approaches for preventing and reducing risks from pollution that threaten human health and the environment. The focus of the Laboratory's research program is on methods and their cost-effectiveness for prevention and control of pollution to air, land, water, and subsurface resources; protection of water quality in public water systems; remediation of contaminated sites, sediments and ground water; prevention and control of indoor air pollution; and restoration of ecosystems. NRMRL collaborates with both public and private sector partners to foster technologies that reduce the cost of compliance and to anticipate emerging problems. NRMRL's research provides solutions to environmental problems by: developing and promoting technologies that protect and improve the environment; advancing scientific and engineering information to support regulatory and policy decisions; and providing the technical support and information transfer to ensure implementation of environmental regulations and strategies at the national, state, and community levels.

This publication has been produced as part of the Laboratory's strategic long-term research plan. It is published and made available by EPA's Office of Research and Development to assist the user community and to link researchers with their clients.

Lawrence W. Reiter, Acting Director.
National Risk Management Research Laboratory

EPA Review Notice

This report has been peer and administratively reviewed by the U.S. Environmental Protection Agency and approved for publication. Mention of trade names or commercial products does not constitute endorsement or recommendation for use.

This document is available to the public through the National Technical Information Service, Springfield, Virginia 22161.

Table of Contents

List of Figures

List of Figures (continued)

Figure **Page**

List of Tables

Abbreviations and Acronyms

Term	Definition
A/C	fabric filter air-to-cloth ratio (also face velocity), fpm
acm	actual cubic meter
Atm	atmosphere
bscat	scattering coefficient
CCM	controlled condensation method for measuring SO_3
D50	particle size at which collection efficiency is 50%
dM/dLogD	derivative of particulate mass concentration by particle size with respect to the logarithm of particle diameter. (Also the slope of the cumulative particle concentration smaller than diameter curve when plotted on a semi-log graph.)
dncm	dry normal cubic meter (Normal conditions are 20 °C at 1 atm.)
dV/dLogD	derivative of particulate volume concentration by particle size with respect to the logarithm of particle diameter.
$d\gamma$/dLogD	derivative of the scattering coefficient by particle size with respect to the logarithm of particle diameter.
EPA	Environmental Protection Agency
EPRI	Electric Power Research Institute
ESP	electrostatic precipitator
FGD	flue gas desulfurization
L	path length
MW	megawatt
Op	opacity
PC	pulverized coal
PCD	pollution (or particulate) control device
PM	particulate matter
ppmv	parts per million by volume
RH	relative humidity
SCA	ESP specific collection area, ft^2/1000 acfm
SCR	selective catalytic reduction
SEM	scanning electron microscope

Abbreviations and Acronyms (continued)

Term	Definition
slip	the amount of ammonia that passes unreacted through an SCR catalyst bed
SRI	Southern Research Institute
γ	scattering coefficient = the total effective particle light-scattering cross sectional area per unit of path length
γ^*	ratio of a particle's effective scattering cross sectional area to its volume
γ^*_{ave}	average specific scattering coefficient over all particle sizes

Identification of (and Responses to) Potential Effects Of SCR and Wet Scrubbers on Fine Particulate Emissions and Plume Characteristics

1. Introduction

Substantial reductions of emissions of nitrogen and sulfur oxides, which are precursors of ambient fine particulate matter, from coal-fired boilers have been accomplished through improvements in combustion practices [such as burners that reduce oxides of nitrogen (NO_X)], application of scrubbers, and increased use of low sulfur coals. Further substantial reductions of these precursors of ambient fine particulate matter will be accomplished by widespread installation of selective catalytic reduction (SCR) systems and additional wet flue gas desulfurization (FGD) scrubbers. These control systems can provide low NO_X and sulfur dioxide (SO_2) emission levels while also relaxing the limitations of fuel sulfur levels. However, observations associated with exploratory research of SCR and FGD technologies and some early full-scale installations reveal some important side effects, which have produced operational and particulate emissions problems of a yet-to-be-determined degree and scope.

The indirect effects of SCR technology on process operation that are of immediate interest center around its catalytic enhancement of SO_2 oxidation to sulfur trioxide (SO_3) which, in turn, reacts through multiple potential paths that can interfere with air heater performance, particulate collection, ash disposal, or balance-of-plant issues. [Although SO_3 vapor is converted to sulfuric acid (H_2SO_4) vapor as temperature declines from 650 to 400 °F, most discussions refer to all forms as SO_3. The present discussion utilizes both terms interchangeably.] Associated particulate emissions impacts of interest are substantial increases of sulfuric acid aerosols, which form in the wet scrubber or in the plume near the stack if a wet scrubber is not present. These condensation aerosols are visible and persist over long distances, in part, due to their particle size and, in part, due to the retention of substantial fractions of water.

The low temperature of wet scrubber effluent produces less plume rise than occurs otherwise with hot stack gas. Furthermore, stacks for use in association with scrubbers are

usually designed to operate at lower gas velocities than those for hotter stack gases in order to minimize entrainment of water droplets from the stack walls. This lower gas velocity further reduces plume rise. Less plume rise leads to higher local, ground-level concentrations of stack gas constituents, relative to plumes formed from hotter stack gas, which rise to high elevations because of high buoyancy. In other words, with lower temperature stack gas (around 150 °F) the degree of dilution that occurs prior to plume contact at the ground is greatly diminished relative to stack gas temperatures greater than 250 °F. Persistent wet FGD scrubber plumes have been observed and referred to as plume blight. Physiological responses such as eye irritation and breathing difficulty have been reported[1] for episodes involving visible plumes containing sulfuric acid aerosols at ground level.

Besides increased visible emissions associated with SO_3, the increased emphasis in recent years on condensable emissions (such as emissions for which EPA Method 202 is utilized) leads to it being counted as a fine particulate emission. Therefore, it may be necessary that contributions of SO_3 aerosols to coal and oil-fired effluent gas produced by SCR installations be taken into account in strategies for satisfying the ambient fine particle standard.

This document summarizes, analyzes, and interprets currently available information concerning SO_3. These results are needed for delineating its impacts on multi-pollutant control strategies to be applied to coal-fired utility boilers for utility and regulatory personnel. It is organized to first review experience with SO_3 prior to and independent of pending changes concerning NO_X and SO_2 control. Parameters that effect its formation in furnaces, interactions with particulate control devices (PCD's), and effects on appearance of stack emissions are discussed. Then SCR characteristics and operating procedures are discussed with emphasis on consistency across the industry. Next, principles of wet FGD scrubbers are reviewed. Concerns with SO_3 measurement and the need and potential for online monitoring are discussed next followed by consideration of SO_3 control. A summary and conclusions are given immediately below.

2. Executive Summary and Conclusions

Due to past experience with SO_3, it was recognized early in the development of SCR technology that catalyst formulations and operating strategies for NO_X control by SCR were needed that kept SO_3 formation as low as practical. Sulfur trioxide formation can be reduced by using a larger volume of catalyst but this increases capital cost. The conversion rate of SO_2 to SO_3, in terms of percent of SO_2, can be specified and achieved with confidence. The uncertainties of SCR operation primarily affect the tradeoffs between ammonia slip (unreacted ammonia that remains in the flue gas downstream of the SCR), NO_X reduction, and the frequency with which one or more catalyst layers must be replaced. In principle, SCRs are operated at a specified minimum level of NO_X reduction that satisfies a systems NO_X compliance strategy, while increasing ammonia injection as needed to maintain the required degree of NO_X control. As the catalyst ages, its NO_X reduction performance degrades, and eventually catalyst must be replaced or additional catalyst must be added. In the latter instance, the added catalyst will result in an increase in SO_3 formation.

Of course, SO_3 catalyzed in an SCR installation adds to that formed in the boiler. Equilibrium favors conversion of SO_2 to SO_3, but it is limited by kinetics to that catalyzed by some of the transition metals, such as iron and vanadium, in the fuel and on boiler tube surfaces. Alkali (alkaline and alkaline earth metals) in the coal counteracts this conversion so that for coals high in alkali, such as most western coals, SO_3 levels exiting the boiler (i.e., exiting the economizer) are low. Indeed, SO_3 levels generated in the boiler are so low with western coals (around 0.1% of the SO_2) that SO_3 is commonly injected upstream of electrostatic precipitators (ESPs) to reduce ash resistivity to levels that allow them to operate properly. Typically, SO_3 conversion rates with low alkali coals are around 1% for pulverized coal (PC) boilers, although as much as 3% is not uncommon. Generally, efficient combustion conditions while minimizing excess air minimizes SO_3 formation. Conversion rates with cyclone boilers burning eastern bituminous coals are about twice that of PC boilers.

Significant losses of SO_3, typically about 50%, occur across air preheaters, the first active system components encountered by the flue gas after an SCR, due to the cool metal surfaces. Much of this loss is the result of condensation on the air heater elements with evaporation into the incoming combustion air returning most of the condensate to the boiler. It is not clear whether the fractional loss is independent of the SO_3 concentration. If the process is diffusion limited, as is believed to be the case, the estimate of 50% loss is applicable to the increase in SO_3 from the SCR. Otherwise the fraction removed may be higher. Additional losses of SO_3 occur across the PCD due to its adsorption by fly ash

particles and condensation onto particles. Typical values of these removal fractions are approximately 50% for ESPs and 90% for baghouses.

Sulfur trioxide reacts with water vapor in the air preheater to become H_2SO_4. There are plant operational concerns with corrosion from acid deposits on air preheater surfaces and in the PCD(s). In addition to corrosion of metal surfaces, bag failure rates in fabric filter installations have been shown to increase as the amount of H_2SO_4 on particles increases. The amount deposited in these devices can be minimized by maintaining flue gas temperatures higher than the H_2SO_4 dew point, but doing so carries a penalty in energy efficiency and may result in a more visible plume.

Effects of ammonia slip on baghouse operation are also of concern. Injection of ammonia at levels of approximately 20 ppmv into flue gas upstream of a baghouse was attempted to extend bag life. It was postulated that the ammonia reaction with H_2SO_4 would prevent acid attack of the fabric. The result was that ammonia injection led to a faster loss of fabric strength than incurred with H_2SO_4 alone. The cause is believed to be formation of ammonium bisulfate, a sticky liquid substance of low pH, formed by reaction with H_2SO_4. It appears that the industry standard for ammonia slip will be 2 ppmv. This standard has evolved to limit ammonia in collected fly ash to avoid interference with its disposal or use as a byproduct.

With this standard, an expected upper limit of 5 ppmv of ammonia (NH_3) is appropriate. These expected levels are significantly less than those found to weaken fabric strength but still high enough to cause concern. In this same test program, injection of a small amount of hydrated lime into the baghouse was found to eliminate the loss in bag strength associated with H_2SO_4 or ammonium bisulfate. Alkali injection removes essentially all SO_3 in baghouses where gas contact with particle surface is high as the flue gas passes through a substantial dust cake. This practice is expected to become common in operation of baghouses to optimize preservation of bag strength after SCR.

Model calculations of aerosol formation for 5 ppmv of ammonia slip and 40 ppmv SO_3 at the exit of an SCR (or air preheater inlet) were performed to predict the size and concentration of particles that would form by reaction of the NH_3 and SO_3. The results indicated that ammonium bisulfate formation dominates over ammonium sulfate (a less sticky solid), and most of it nucleates to ultrafine (less than 0.2 μm diameter) particles that exit the air preheater. These ammonium bisulfate particles would cause a substantial increase in the concentration of sub-micrometer particles entering any downstream PCD.

A computer model of ESP performance[2,3] was then used to estimate the effect of these added particles on net particulate emissions. The model was used to predict emissions from a unit that employed a typical cold-side ESP for particulate control by assuming the ammonium bisulfate aerosol component was added to a typical coal fly ash ESP inlet particle size distribution. The ESP model results showed that space charge would be substantially affected by the amount of added ultrafine aerosol predicted by the aerosol formation model, and the ESP current would decrease significantly for a given applied voltage prior to SCR installation. However, since installation of an SCR will lead to a net increase in SO_3 entering the ESP, fly ash resistivity would be at least as low as it was prior to SCR installation and probably would be lower. Therefore, the applied voltage could be increased, depending on the power supply limitations, to reinstate the ESP current. This would result in a slight net improvement in collection efficiency. The opacity of the exit stream was predicted to decrease from 11% before SCR installation to 9% afterward for the case modeled. Instances of field observation of improved ESP performance with NH_3 injection have been reported.[4]

The levels of ammonia slip considered here, for which no degradation of ESP performance is indicated, are expected to be representative of most SCR installations. If NH_3 and SO3 levels present at the air preheater inlet are allowed to be substantially larger, then other factors should be considered. Tests performed in the field have included conditions in which NH_3 injection led to deposition of ammonium bisulfate particles on collection plates and corona electrodes leading to enough particulate build-up to interfere with ESP performance. Thus, ESPs downstream of SCRs should be monitored for any hints of long-term degradation due to accumulation of ammonium bisulfate on corona and plate electrodes that are not removed by normal rapping.

Removal of SO_3 in wet FGD scrubbers is thought to be low because consideration of aerosol formation mechanisms suggests that it forms a submicrometer mist at scrubber inlets. This conjecture has been borne out by measurements. In a number of instances, more particles having diameters around 0.1 μm have been found at scrubber outlets than at the respective inlets when SO_3 was present in the inlet gas stream.[5] The apparent cause is a rapid quenching of the SO_3 bearing flue gas, leading to nucleation and formation of ultrafine particles. In addition, persistent scrubber plumes are most frequently associated with flue gas streams known to have SO_3. In spite of the predicted low collection efficiencies of these ultrafine particles, attempts at direct measurement of SO_3 removal using current methods indicate significant collection, typically in the range of 30% to 80%.[6] As discussed below, there are good reasons to question SO_3 measurements at scrubber outlets. As a result, actual collection efficiencies of SO_3 by scrubbers should be considered to be poorly quantified, and

reported values over 50% should be considered especially suspect. Measured particle collection efficiencies over the relevant particle size range for low energy scrubbers (or low-pressure loss, 1" to 2" H_2O) utilized for FGD are not available, although scrubber D50 (size at which collection efficiency is 50%) is typically around 4 μm. Review of measured particle collection efficiency over the relevant particle size range for high energy scrubbers often indicates that some collection, albeit well below 50%, is achieved at all sizes below the D50.

The inconsistent measurements of SO_3 removal efficiency indicated above were obtained using the controlled condensation method (CCM). Since the early 1980's, this method has been widely believed to produce the most accurate results for SO_3 measurement at the concentrations encountered in flue gases from coal-fired boilers. The CCM method was developed primarily for measurement of vapor phase SO_3. However, current needs are for measurement of total vapor and particulate phases. It is widely believed that much of SO_3 present in the exit gas stream of air preheaters and beyond is adsorbed to fly ash. Further, alternate, experimental measurements using cascade impactors for SO_3 downstream of scrubbers have, on occasion, shown substantial acid levels in particles having diameters larger than ten micrometers. These results suggest substantial particle growth, driven by the huge capacity for water by sulfuric acid, can qualitatively be expected in moisture-saturated gas, such as that in exiting scrubbers if the gas has sufficient residence time for growth by diffusion. The presence of acid incorporated with particles larger than a micrometer could explain the inconsistent SO_3 results by CCM downstream of wet FGDs as these may not be sampled correctly by the CCM method. On the other hand, the inconsistent results may be caused by reaction with droplets of scrubber liquor in the CCM sampling probe.

Considering the mechanisms for producing SO_3 and removing it from flue gas, it is obvious that the appropriate design specification for conversion rate from SO_2 to SO_3 in a given SCR is specific to parameters of the boiler and the other components of the effluent gas stream. For boilers using low to medium sulfur coal (less than 1.5% sulfur) the typical conversion rate specifications for SCRs are in the 0.5% to 1.5% range. It is expected that 0.5% to 0.75% will be selected for many of those boilers using high sulfur coal except, perhaps, for those for which explicit removal systems for SO_3, discussed below, are available. Note that these specifications refer to levels expected after SCR catalysts have been in service to the extent that all design catalyst layers are installed. Actual levels of conversion are expected to be close to, but below, the specified levels.

Given the regulatory impetus expected from various proposed new laws and rule-making

regarding pollutant emissions (Clear Skies, Mercury Rule, and Interstate Air Quality Rule), the use of wet FGD scrubbers is expected to become widespread over the next 5 to 10 years. As a result, stack plumes will generally be at lower altitudes due to lower stack exit velocities and reduced plume temperature and buoyancy. Thus, under certain conditions, the plume will contact the ground near the stack (occasionally within 1 mile and more frequently within 5 miles). In that type of circumstance, characterization of the plume appearance in terms of opacity, as is normally used for source emission, is not reliable. There would be great uncertainty and variability of an appropriate path length (plume diameter) through which an observer would view the plume and, of course, occasionally an observer could be in the plume. Characterization of ambient air frequently uses the scattering coefficient (meters to the minus one) parameter[7], which is also a part of opacity considerations, to quantify the appearance (light scattering) of ambient aerosol. In the ambient air context this term is called “bscat.”

There are two features about visual observations of stack emissions that are relevant: attenuation of light passing through the plume as measured by opacity and light scattered from all directions incident on the plume into the direction of the observer. When below 5% to 10%, opacity is difficult to measure quantitatively and becomes an insensitive monitoring parameter. Scattered light is still readily visible when opacity is below levels of its usefulness for monitoring. It is common with modern, large particulate control technology that opacity is well below 10% so that the plume appearance is dominated by scattered light. Therefore, this effort has focused on scattered light although the measure of it is the same as addressed in opacity concerns. Light absorption by coal-fired boiler ash is rarely significant, so scattering is the normal cause of opacity.

The effects on fine particle and visible emissions by the numerous factors involved in SCR and wet FGD scrubbers are illustrated in Table 1. The quantities in the table are based on typical values currently available for the listed production and removal mechanisms. These results are presented assuming no specific efforts at controlling SO_3 beyond current practice and low alkali coal. The conditions of the various effluent gas streams that were considered are listed in the first column. The next five columns present levels of SO_3 expected to exit each of the components of those streams using the assumptions of typical conversion rates (SO_2 to SO_3) and removal efficiencies (as provided in the footnotes to the table). The three levels of coal sulfur considered—low, medium, and high—correspond to assumed values of 800, 1500, and 3000 ppmv SO_2 produced from the coal. The seventh column lists the corresponding fine particulate matter (PM) expected to be emitted derived from the mass concentration of H_2SO_4 per ppmv (4.03 mg/dncm per ppmv at dry normal conditions). This

value does not count water that combines with H_2SO_4 in PM measurement methods. Since the rates of SO_2 to SO_3 conversion considered are coincidentally both one percent for boiler and SCR production, half of the fine PM shown represents an increment associated with SCR.

In order to characterize the effects of SO_3 on the appearance of emissions in this analysis, the scattering coefficient was resolved into two additive terms: the scattering coefficient for PM not associated with SO_3 and that associated with SO_3. Table 1addresses only the latter. (The appearance of the emissions will also be affected by the emissions of fly ash and NO_X.) The scattering coefficient of an aerosol is determined by both its concentration and particle size distribution. For the purposes of Table 1, the SO_3 contribution to the scattering coefficient was resolved into two factors: acid (H_2SO_4 and combined water) volume concentration and the average specific scattering coefficient. The latter was quantified separately based on estimated particle size and refractive index. The value of this size dependent component is determined by aerosol formation and growth mechanisms. These, in turn, depend on temperature conditions and the concentrations of H_2SO_4 and water. The mechanisms include nucleation, heterogeneous condensation onto preexisting fly ash, and coagulation. For hot stack effluents, consideration was given to both modeling and field data derived from air-dilution sampling systems to quantify the average specific scattering coefficient under two scenarios: (1) that in which heterogeneous condensation dominates (higher values given in the table notes) and (2) that in which homogeneous nucleation dominates. The latter case is associated with relatively low fly ash loadings presenting relatively little particle surface area.

For stack effluents from wet FGD systems, the average specific scattering coefficient was calculated based on estimated lower limits for concentrations by particle size resulting from nucleation followed by coagulation. These estimates simulate nucleation of acid at the inlet of a wet FGD and the coagulation that follows as a function of residence time in the scrubber and stack. Residence time in the scrubber and stack is assumed to be 20 seconds for Table 1. These results are presented in more detail later in Section 5 of this report. The amount of water included with H_2SO_4 was 65% by weight of the two combined components. This weight percentage corresponds to ambient conditions of 20 °C at 70% relative humidity (RH). Acid droplets in a scrubber plume will reach those conditions in ambient air, but while in the scrubber and stack, where the RH is 100%, the amount of absorbed water is much larger even though the temperature is about 60 °C. Thus, these droplets actually grow by absorption as well as coagulation. A larger droplet diameter enhances coagulation somewhat, so it is expected that the actual size would be somewhat larger in diameter and

Table 1. Illustration of Potential Effects of SO_3/H_2SO_4 on Fine Particle Emissions and Visible Emissions

Coal Type and Control Devices	H_2SO_4 Concentrationa Exiting Effluent Stream Components (ppmv)					H_2SO_4 Fine PM Emissions (mg/dncm)	H_2SO_4 Contribution to Plume Scattering Coefficient[a] (m^{-1})		
	Boilr[b]	SCR[c]	Air Perhtr[d]	PCD[e]	Wet FGD[f]		Near stack[g]	Int. med[h] ($\times10^{-5}$)	Dist[i] ($\times10^{-5}$)
Low sulfur, ESP only	8	NA[k]	4	2	NA	8	0.006		0.4
Low sulfur, ESP only & low fly ash[j]	8	NA	4	2	NA	8	0.002		0.1
Medium sulfur, ESP only	15	NA	8	4	NA	15	0.011		0.7
Medium sulfur, ESP only & low fly ash[j]	15	NA	8	4	NA	15	0.004		0.2
High sulfur, ESP only	30	NA	15	8	NA	31	0.022		1.4
High sulfur, ESP only & low fly ash[j]	30	NA	15	8	NA	31	0.007		0.5
Low sulfur, ESP & SCR	8	8	8	4	NA	16	0.012		0.8
Low sulfur, ESP, SCR & low fly ash[j]	8	8	8	4	NA	16	0.004		0.2
Medium sulfur, ESP & SCR	15	15	15	8	NA	31	0.022		1.4
Medium sulfur with ESP, SCR & low fly ash[j]	15	15	15	8	NA	31	0.007		0.5
High sulfur, ESP & SCR	30	30	30	15	NA	61	0.045		2.9
High sulfur, ESP, SCR & low fly ash[j]	30	30	30	15	NA	61	0.014		0.9
Low sulfur, ESP, SCR & wet FGD	8	8	8	4	3	11	H_2O fog	3.1	0.3
Medium sulfur with ESP, SCR & wet FGD	15	15	15	8	5	21	H_2O fog	10.5	1.0
High sulfur, ESP, SCR & wet FGD	30	30	30	15	11	43	H_2O fog	37.7	3.8

[a] For reference, the scattering coefficient of clean ambient air is 10^{-5} m^{-1} and a value > 24×10^{-5} m^{-1} is considered an adverse condition[7].

[b] Alkali typical of eastern coals with SO_3 production in convection sections of boiler ≈ 1% of SO_2.

[c] SO_3 production in SCR. SO_3/SO_2 ratio ≈ 1% for all sulfur levels (Note: the ratio will be about 0.75% for many boilers using high sulfur coals).

[d] Air preheater H_2SO_4 removal ≈ 50%.

[e] ESP H_2SO_4 removal ≈ 50% or baghouse ≈ 90%.

[f] Wet FGD scrubber removal ≈ 30%.

[g] Hot stack plume (without wet FGD); temperature of 60 °C, water vapor volume fraction of 3%, combined water ≈ 35% by weight, 45% by volume. Particulate volume of H_2SO_4 is 0.00362 cm^3/m^3/ppmv. The expected range of average of the specific scattering coefficient is 0.2 to 2.5 m^2/cm^3. Estimated here as 2.07 and 0.66 respectively for submicron fly ash loadings that are typical (>2 mg/dncm) and low (<2 mg/dncm). Effluent gas diluted by 2.5. To convert value to opacity multiply by 2.5 × stack diameter (in meters).

[h] With scrubber, temperature of 20 °C, water vapor volume fraction of 1.5%, combined water ≈ 65% by weight, 76% by volume. Particulate volume for H_2SO_4 is 0.00925 cm^3/m^3/ppmv. Estimated average specific scattering coefficient given by $\gamma^*ave = -0.0078\bullet[H_2SO_4, ppmv]^2 + 0.4514\bullet[H_2SO_4, ppmv]$, effluent gas diluted by 1000.

[i] Same conditions as Note “h” except flue gas diluted by 10,000. Estimated average specific scattering coefficient of Note “f “ (without scrubber) and of Note “g“ (with scrubber).

[j] Low fly ash refers to low submicron loadings (< 2 mg/dncm). All other submicron loadings >> 2 mg/dncm. See Note “g.”

[K] NA = not applicable.

have correspondingly larger average specific scattering coefficients. For example, under these conditions (see Section 5), it has been shown that average specific scattering coefficients follow a quadratic in H_2SO_4 concentration with coefficients which depend upon the residence time in the scrubber and stack, 20 s for the current example.

The results given in Table 1 illustrate how the relevant variables, primary and secondary, contribute to the overall fine PM mass and appearance of PM emissions. Since the values for each individual variable are estimates of typical values, the frequency with which the indicated results occur cannot be predicted. However, to interpret these results, it is useful to compare them to general observation as some gauge as to the quality of the estimates. In addition, the circumstances for which there need not be much cause for concern may be indicated. Table 1 suggests that installation of SCR will increase opacity (product of near stack scattering coefficient and plume diameter). Considering installations without wet FGD, if a very efficient ESP is used for particulate control, so that fly-ash submicrometer loadings are low, thus promoting nucleation, the estimated opacity increase ranges from 1% to 8% as coal changes from low sulfur to high sulfur. With higher fly ash loadings, the corresponding estimated range of the increase is from 4% to 19%. This potential increase should be considered in choosing an SCR specification for SO_2 conversion rate or in considering separate SO_3 removal in conjunction with SCR installation. Assistance in those deliberations can come from pilot tests at the site using air-dilution sampling systems (also called plume simulation sampling systems) that mimic the processes that take place in the plume near the stack together with comprehensive modeling. Sites that burn high alkali coals or that use a baghouse for the PCD will likely experience essentially no change of emissions.

Because wet FGD scrubber effluents can contact the ground relatively close to the stacks, installation of a scrubber (without SO_3 removal) could lead to haze on the ground within several miles of the plant. The column labeled “Intermediate” represents an occasion when wet FGD plume contacts the ground at a distance on the order of one mile from the stack when dilution has progressed to 1,000. The results suggest that haze would result at this location when firing a high sulfur coal. Note the reference point concerning appearance given in Note “f” of Table 1. For lower sulfur coals, the impact would be marginally noticeable from a visual perspective. At “Distant” locations, no haze is predicted for low sulfur based upon the estimates of typical values presented here. In the distant plume, all conditions considered here lead to scattering coefficients that are near clean air conditions except “High Sulfur with ESP & SCR.” Consideration of the order of magnitude of the results suggests the potential importance of variations of variables from the typical values.

For example, if most of the variations in SO_3 production and removal rates were in the direction to increase SO_3, then a very different picture emerges in which environmental impact could be more substantial.

In those cases in which plume blight from SO_3 is expected to be a problem, each of four general approaches provide a high probability for successful SO_3 removal: (1) alkali injection into the furnace, (2) humidification at an ESP inlet to reduce the temperature to below the acid dew point, (3) alkali injection combined with humidification at the ESP inlet, and (4) a separate wet particulate control device such as a wet ESP. All of these approaches have been tested in demonstration scale, but all must be considered new technology that will require adjustments or identifications of procedures to deal with specific sites. The first three have balance of plant issues associated with them; that is, increase risks of unforeseen negative effects on plant operation. Other concepts of interest, but less fully tested, include (1) alkali injection in ducting leading to a wet FGD scrubber and (2) an electrostatically augmented mist eliminator. Various devices are also being offered which have the purpose of contacting sorbents with flue gas for removal of other gaseous pollutants as well as SO_3.

3. Conventional Experience with SO_3 (without SCR or Wet FGD)

SO_3 Formation in Boilers

The formation of sulfuric acid in a boiler occurs when a small fraction of the sulfur in the fuel is oxidized beyond SO_2 to SO_3, which subsequently reacts with water vapor to form H_2SO_4. Almost all of the sulfur is oxidized to SO_2 in the combustion zone; indeed, at high temperature, SO_2 is the equilibrium form. As the gas temperature falls between the combustion zone and the stack plume, shifts in the equilibria occur, illustrated in Figure 1, from SO_2 (gas) ⇒ SO_3 (gas) ⇒ H_2SO_4, (gas) ⇒ H_2SO_4-H_2O (liquid). Thermodynamically, SO_2 is the most stable species in the combustion zone; SO_3 is the most stable species in the intermediate-temperature zone between the economizer and air preheater; sulfuric acid vapor is the most stable species between the air preheater and the stack or wet scrubber (if present); and diluted liquid sulfuric acid aerosol is the most stable species in the wet scrubber and stack effluent. Of course, the levels of these species other than SO_2 are much lower than that of SO_2 itself, which remains the predominant fraction of the sulfur present due to kinetic factors that limit the key oxidation step from SO_2 to SO_3. Therefore, in addition to fuel sulfur and excess combustion air levels, the rate of formation of SO_3 depends on catalytic oxidation associated with some metals in the ash and on the boiler tube surfaces, especially iron and vanadium.[8,9,10,11] Coals also contain alkaline metals, especially calcium, sodium, and magnesium, that can react with and limit the net sulfuric acid as illustrated in the lower right of Figure 1.

Reported boiler oxidation rates for SO_2 to SO_3 run as high as 5% of the SO_2 for coal-fired boilers[8] and 10% for residual oil-fired boilers[9,12], while typical rates for low alkali coals are near 1%.[8] When one considers utility boilers burning eastern 3%-sulfur fuels that produce SO_2 levels greater than 2000 ppmv, quite high levels of SO_3 or H_2SO_4 might be encountered, but typical levels are much lower due to several factors associated with plant operation. These factors include minimization of excess air, control of boiler tube fouling, fuel selection, and other plant operating procedures applied to limit corrosion, sulfur emissions, and visible emissions associated with condensed sulfuric acid.

Walsh et al. measured SO_2 oxidation by the vapor phase homogeneous reaction at the furnace exit of a stoker boiler to be 0.9% and suggested this observation to be near an upper limit set by the SO_3/SO_2 equilibrium at high furnace temperatures.[12] Graham and Sarofim estimated this uncatalyzed contribution at 0.5% for a pulverized coal (PC) boiler.[10]

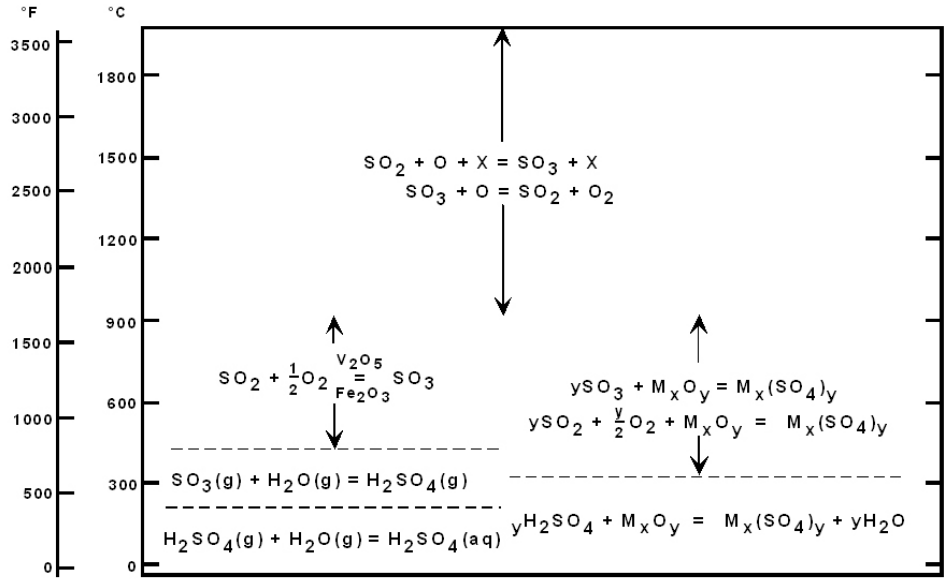

Figure 1. Processes contributing to formation of sulfur trioxide, sulfuric acid, and sulfates. After Walsh.[11]

Interaction of SO_2 with catalytic compounds and SO_3 with alkaline compounds involves gas interfacing with boiler tube surfaces, with bare metal or deposited ash, or with suspended (aerosolized) fly ash. Walsh, et al. investigated catalysis of SO_2 to SO_3 by iron in and on the boiler tubes considering clean tubes, tubes fouled with coal fly ash, and the combination. Their calculations from first principles suggest a range of conversion rates from 1% to 5% depending on the degree of tube fouling and amount of iron in the coal ash.[12] Tube fouling led to higher surface temperatures of deposited ash, thus enhancing the rate of catalysis by Fe_2O_3 present in the ash, 13% of the ash mass in the instance studied. Clean tubes led to lower tube surface temperatures and limited catalysis to lower rates, but the amount of available iron was higher at the clean tube surface. The 1% (lowest) value of calculated conversion rate corresponded to no tube fouling, and the heavy tube fouling condition resulted in a 2% value. The 5% (highest) value corresponded to combined clean and fouled tubes.

The modeling results by Walsh et al.[12] for catalytic conversion associated with iron in suspended fly ash particles was 0.3%. If applied to PC boilers, this modeling result for suspended fly ash would be substantially higher. That conclusion follows from the apportioning of ash between bottom ash and flue gas typical for PC boilers, 20%/80%, versus that for stoker boilers, 90%/10%.

Although Walsh, et al.[12] conclude a total conversion rate as high as 6% for SO_2 to SO_3, measurements showed that two-thirds of it was removed in transit to and through the economizer of the boiler. Uptake by ash particles, by processes other than simple condensation, was suggested as the mechanism for SO_3 removal. Graham and Sarofim[10] investigated sulfation by alkaline metals in the ash as an important mechanism that limits SO_3 exiting PC boilers. The importance of alkaline metals was illustrated by referencing results from a laboratory study by Neville[13] as shown in Table 2. The variation in conversion rate over coal type from 8.9% with Western Kentucky coal down to negligible net conversion for Montana lignite was explained in terms of competition between catalytic activity by iron oxide and subsequent sulfation by alkaline metal oxides, especially calcium, sodium, and magnesium in coal. These net conversion rates are considered only as upper limits for these coals because of the high oxygen levels utilized in this laboratory study.

Table 2. Conversion of coal sulfur to sulfuric acid and inorganic sulfate.[a]

Coal Type	Coal Sulfur (%)	Sulfur Converted to Sulfuric Acid (%)	Sulfur Converted to Inorganic Sulfate (%)
Alabama Rosa	0.85	3.4	2.8
Illinois #6	4.1	6.2	2.17
Montana Lignite	0.55	0.	34.3
PSOC - 3[b]	0.69	4.7	1.6
PSOC - 26[b]	3.95	4.1	1.4
Western Kentucky	3.15	8.9	1.4

[a] Laboratory coal study; combustion conditions: 75% oxygen, furnace temperature = 1200 K.

[b] From the Pennsylvania State Coal Sample Repository.

The data showing sulfur converted to sulfuric acid in Table 2 were derived from pH data of distilled water after adding freshly generated coal ash that was collected at low temperature relative to the acid dew point. The pH of the water decreased rapidly to a minimum in about 2 minutes and then rose substantially over a period of a few hours. The sulfuric acid condensed or adsorbed on the ash was calculated from this minimum pH. The subsequent rise in pH was caused by the dissolution into the distilled water of alkali components in the fly ash. In similar experiments measuring sulfuric acid on fly ash from a coal-fired boiler burning 3% sulfur Eastern bituminous coal, it was found that after the pH dropped to levels below 4, it rose in about 10 minutes to levels over 11.[14] Thus, perhaps there is more than

enough alkaline material in a given fly ash to neutralize formed acid, but the amount located on the fly ash surface structures may not be sufficient to fully neutralize it.

Due largely to the abundance of alkaline metals in Western coals, SO_3 formation is dramatically lower than for low alkali, Eastern bituminous coals. Hardman et al.[8] identified three categories with SO_2 to SO_3 conversion rates that correlate inversely with levels of alkaline metals. A recent update of that initial investigation added lignite as a fourth category.[15] The estimated values offered by these authors are 0.008 for Eastern bituminous, 0.001 for Western bituminous, 0.001 for lignite, and 0.0005 for Western subbituminous coals when burned in PC boilers. In addition, this latter investigation concluded that cyclone boilers have conversion rates about double those of PC boilers.

Ash Particle Size Components

The degree of interaction of SO_2 with catalytic compounds and of SO_3 with alkaline compounds is related to a set of processes that determine the distribution of compounds by particle size in fly ash exiting boilers. These processes are the nucleation, condensation, and coagulation of vapor-phase species in the presence of other particles or droplets suspended in the flow. These processes are included in this discussion because they affect not only the vapor-phase SO_3 concentration in the boiler effluent gas stream but also subsequent conversion to particulate sulfate components that subsequently affect if and where these sulfate components are removed in any given flue gas stream. In the boiler the relevant compounds are the metal species formed from vaporized ash constituents.

Figure 2 illustrates typical particle size distributions for fly ash entering and leaving an ESP controlling emissions from a PC boiler. The ESP inlet measurements were obtained by combining results from a University of Washington Mark III cascade impactor operated in-situ (for concentrations at sizes above 0.5 μm) and a TSI Scanning Mobility Particle Sizer (Model 3934) with extracted, dried, and cooled sample gas (for concentrations at sizes below 0.7 μm).

Metal oxide fume is formed from metal atoms and metal oxides generated in the high temperature reducing environment of burning char residues in pulverized coal flames (Quann and Sarofim,[16] Senior and Flagan,[17] and Helble et al.[18]). (Char is the remains of a solid carbonaceous fuel that has been incompletely combusted, such as charcoal if wood is incompletely burned.) Metal oxide fume is the principal source of the typical ultrafine particle mode (peak) centered around 0.1 μm as illustrated in Figure 2. The latter is an example typical of observed particle size distributions and loadings of coal fly ash exiting

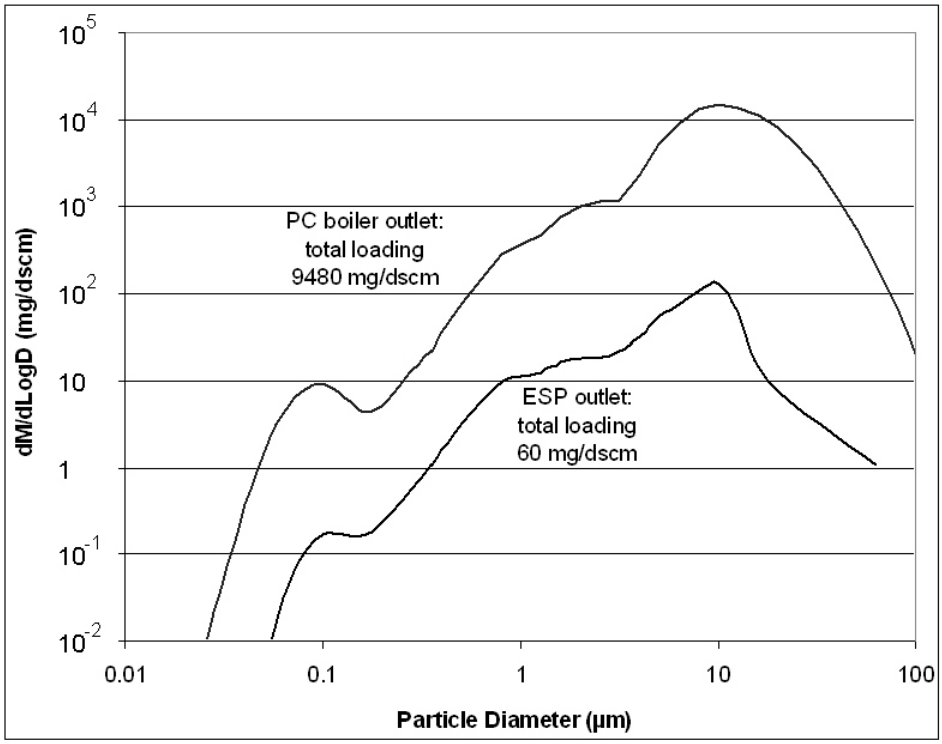

Figure 2. Particle size distributions of fly ash exiting a pulverized-coal-fired (PC) utility boiler. (The outlet size distribution was calculated from the measured inlet distribution using an ESP model applied to a typical ESP setup at typical flue gas conditions with 1% sulfur, Eastern-bituminous coal.)

tangentially-fired PC boilers. These data were obtained during combustion of Eastern bituminous coal with 0.8% sulfur. Iron, calcium, and magnesium are among the elements vaporized from ash during combustion of bituminous coals (Quann and Sarofim[16] and Helble et al.[18]). Iron oxide is an effective catalyst for oxidation of SO_2 to SO_3; therefore, the particle size distribution and surface area of iron-containing particles are of some importance in determining the conversion of SO_2 to SO_3 in the convection section. Finely divided calcium and magnesium oxides are effective sorbents for SO_3 and H_2SO_4, so a shift of these elements to smaller size is likely to reduce the concentration of free acid (Graham and Sarofim[10]).

The vaporization of inorganic species from burning char was treated in detail by Quann and Sarofim.[16] In their mechanism, volatile metal atoms and metal suboxides are produced by

reduction of the full oxides by carbon monoxide inside the char. On leaving the char, these vapor species encounter a more oxidizing environment and return to their normal oxidation states, which have extremely low vapor pressures. The products of this reaction are, therefore, supersaturated and homogeneously nucleate to form nanometer-size particles of the solid metal oxides, such as Fe_3O_4, CaO, and MgO. These ultrafine primary particles grow by coagulation in the boundary layers of char particles and in the free stream during the passage of combustion products through the furnace, approaching a mean size in the 0.1 to 0.3 μm range that are characteristic of the accumulation mode.

Combustion, and the processes described above, generate a particle size and composition distribution at the furnace exit consisting of three major components: (1) unburned char particles having sizes of the order of 100 μm, (2) ash particles having sizes on the order of 10 μm that are formed from extraneous mineral particles in the fuel and ash released during burnout of the char, and (3) fine particles formed by nucleation, condensation, and coagulation of the most volatile inorganic elements in the ash, as described above. Depending on coal type and ash composition, iron, calcium, and magnesium may be present in both the large ash and fine particles. The char may have high internal surface area and absorb sulfuric acid at low temperatures. Coagulation and growth of submicrometer particles continues in the convection section, possibly with small additions to their mass from condensation of volatile trace metals as the flue gas is cooled. Superimposed on this complex system are the losses of vapor species, fine particles, and coarse particles by condensation, thermophoretic transport, and inertial impaction, respectively, to heat transfer surfaces in the convection section.

In laboratory simulations Graham and Sarofim[10] investigated the portion of SO_3 formation and sulfation of alkaline compounds associated with the fine aerosol ash component in boilers. Based on projections to PC boiler conditions of laboratory measurements of catalytic rates by 0.1-μm Fe_2O_3 particles, the condensed iron component (in the fine mode) of fly ash was estimated to contribute a 0.5% conversion rate for typical PC boiler conditions. This particle size mode presents the most effective catalysis per unit mass of iron but contains a small fraction of the total iron. The authors' calculations addressed only the Fe_2O_3 ash fraction found in the sub-micrometer mode of the size distribution, which represented only 0.5% by weight of the total fly ash while typical Fe_2O_3 ash fractions range from about 5% to 20% of the total fly ash. The authors characterized typical total conversion rate of SO_2 to SO_3 as 1% to 3%, including that occurring at heat transfer surfaces and other particles making up the total of the fly ash. In addition to catalytic oxidation by Fe_2O_3 particles, Graham and Sarofim[10] measured sulfation rates by 0.015 μm CaO particles. Based

on the measured rates, ranging from 10^{-7} to 3×10^{-6} moles CaO/m^{2}s over temperatures from 400 to 600 °C and up to 1.5×10^{-3} at 1000 °C for 3000 ppmv SO_2 and 5% O_2, it was concluded that all such particles in this size mode are sulfated at typical PC boiler conditions. However, for the current context of impact on SO_3 levels, it is not clear how much of the sulfation occurs in reaction with SO_2 rather than SO_3.

Air Preheaters

Substantial reduction in SO_3 and/or sulfuric acid is common across air preheaters where the average gas temperature decreases from about 650 to 325 °F. Dew point curves are given in Figure 3. High losses by condensation on metal surfaces are readily understandable qualitatively, considering these dew point data combined with the fact that the average metal surface temperature varies from about 140 to 270 °F across the plane located at the last 0.3 m of a rotary-regenerative preheater basket.[19] SO_3 levels downstream of air preheaters are typically observed to be significantly below the acid dew point levels corresponding to the average flue gas temperature. Several investigators suggest reduction of SO_3 across air preheaters when burning Eastern bituminous coal by a factor around 50%.[8,15,19,20] With other coals, for which much less SO_3 is produced in the boiler, one available estimate is 10%.[15] DeVito and Oda[20] reported results of parallel SO_3 measurements at a preheater flue gas inlet and outlet and in the combustion-air side of an air preheater. They found that the 40% of the SO_3 entering the air preheater was removed from the flue gas and attributed it to condensation of H_2SO_4 onto the air preheater surfaces.[20] Measurements performed in the combustion air stream passing through the air preheater on its way to the furnace led to the conclusion that H_2SO_4 removed from the flue gas was revolatilized in the combustion air stream.

In passing through air preheaters, flue gas temperatures decrease through the range in which SO_3 is converted to H_2SO_4. Significant portions are in both the particulate and vapor phases as reflected by observations of ash pH like those discussed above and by the inverse dependence of fly ash resistivity on SO_3 as characterized by investigations of ESP operation.[21] Zhang[22] performed fundamental calculations (for rotary-regenerative preheaters) of both H_2SO_4 vapor condensation on wall surfaces and transfer to suspended particulate matter by homogeneous nucleation, heterogeneous condensation, and adsorption by fly ash. All of these mechanisms were found to contribute significantly to the fate of SO_3.

The analysis of Hardman and Dismukes[8] reported above, characterizing SO_3 levels, was based upon empirical data at the air preheater exits of 18 conventional PC boilers. Coefficients of variation of these field data were around 50%; from this, one can surmise

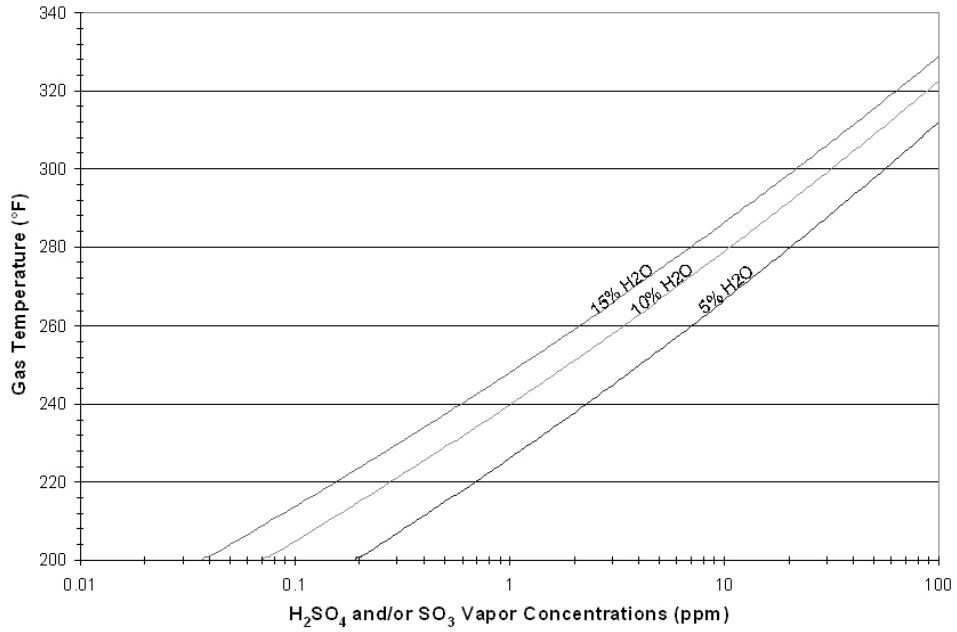

Figure 3. Dew point curves for gas containing different concentrations of water vapor at total pressure of 1 atm.[23]

that levels a factor of two higher or lower than the typical values used in the present analysis are not unusual. For example, with SO_2 levels greater than 2000 ppmv (resulting from the use of Eastern bituminous coal), 4 to 16 ppmv of SO_3 or H_2SO_4 could be expected at air preheater exits of PC boilers. Higher and lower levels cannot be ruled out because of the uncertainty associated with catalytic oxidation and sulfation in boilers or varying losses in the air preheater. Indeed, these conditions and higher variations from the norms of SO_3 values have been observed at some sites over three decades of investigation.

Improved Electrical Resistivity and Cohesion in Electrostatic Precipitators

Many electrical utility plant operators have long dealt with the presence of sulfuric acid. Some level of acid aerosol has been found to be beneficial because condensed or adsorbed acid reduces fly ash resistivity, resulting in more nearly optimum ESP performance. In fact, for many units burning low sulfur coal, especially those burning western coals with high alkali levels, SO_3 is injected upstream of the ESP to improve collection efficiency by reducing resistivity. However, the dependence of resistivity on SO_3 level is subtle. It has been found that, to be accurate, the empirical relationship developed for fly ash resistivity requires as input data the concentrations of nine common metals plus sulfate in the ash as well as SO_3 concentration, moisture content, and temperature of the flue gas.[24]

In addition to reducing resistivity, sulfuric acid condensed or adsorbed on the fly ash can also be beneficial in reducing ESP rapping reentrainment by increasing particle cohesion. Air preheater flue-gas exit temperatures are usually kept high enough to limit levels of condensed-phase acid (see Figure 3), thus both minimizing corrosion rates in, and downstream of, the air preheaters and maintaining the basically dry particulate properties necessary to insure adequate removal of collected particulate matter from ESP corona wires and plates by rapping.

Essentially all of the particle phase acid is removed in the ESP. The fraction that passes through the ESP as vapor varies widely due to the variation of gas temperature in the ESP and variation of acid adsorption/reaction with fly ash composition and temperature. Hardman and Dismukes[8] estimated 25% of the acid exiting the air preheater is removed by cold-side ESPs, but a recent update of that review[15] resulted in an estimated 50% removal.

Baghouses

Performance and operating characteristics of fabric filters differ significantly between units burning low sulfur, high alkali Western coals and high sulfur, low alkali Eastern coals. The difference is such that separate and parallel research facilities were needed to concentrate on each type of flue gas.[25] Sulfuric acid (or SO_3) level is the most important variable associated with observed differences.

A strong tendency toward heavier residual dust cakes is associated with high sulfur coal. Abundant sulfates in the residual dust cake implicate SO_3 in the formation of these cohesive, tenacious dust cakes. Residual dust cake weights of 1 lb/ft^2 (100 lb/bag) were encountered in some high-sulfur coal baghouses.[26] This bag weight is a factor of 20 times the weight of dust accumulated during a single filter cleaning-cycle.[27] In one of these extreme cases, the heavy residual dust cake exceeded the mechanical design capacity and caused failure of the bag suspension mechanism.[28] High residual dust cake weight is the result of high particle cohesion and adhesion. Comparison of scanning electron micrographs (SEMs) of dust cakes from a Western low sulfur subbituminous coal and an Eastern high sulfur bituminous coal revealed the presence of cementitious structures in the latter that did not appear in the former. This term, cementitious structure, was ascribed to contiguous material bridging fly ash particles together and believed to be the cause of enhanced cohesion.[29] Qualitative analysis by the SEM indicated that this bridging material was composed of more sulfur and less of other metals than individual fly ash particles. Separate analyses of dust cake samples and hopper samples showed up to a factor of 5 higher levels of soluble sulfate in the dust cakes. (That is, the residual ash that was not removed from the bags by the normal cleaning

process had a much higher sulfur content than that which fell into the hopper during cleaning).[29] These observations implicate condensed sulfuric acid as the probable cause of the increased cohesion. In addition to the observed correlation of residual dust cake weight to sulfur in the ten coals, it inversely correlated with both sodium and calcium.[26]

Higher residual dust cake weights after cleaning have a positive correlation with more SO_3. However, when normalized for differences in gas flow rate and dust cake thickness, the pressure drops are lower by a factor of 3 to 4 compared to normalized pressure drops in low-sulfur coal fabric filters. It follows that the dust cake collected in the presence of SO_3 forms a more porous structure.[26] Thus, lower pressure drops are often seen in high-sulfur coal fabric filters even though residual dust cakes are much heavier than in low-sulfur installations.

Woven fiberglass is the material of choice for bag construction. The fiberglass yarn is coated with a finish that is intended to protect the yarns from abrasion. The finish may also provide some protection from acid attack. Some yarn finishes have been offered specifically for resistance to acid. High dust cake weights add significant stress to bag fabric. More energetic means of cleaning bags, instead of the predominate method of reverse gas, have been investigated to reduce residual filter cake weights (specifically, sonic horns and shake/deflate), but these also add stress to the filter fabric.[27]

Fabric strength is characterized by the Mullen Burst Strength, a fabric property that is measured by the method specified in ASTM D3786. The test measures the ability of a fabric to resist rupture as the result of pressure exerted by a hydraulically inflated diaphragm.[30] Research has correlated specific bag failures with the loss of fabric strength as measured with the Mullen Burst Strength test.[31] The loss of fabric strength was attributed to the condensation of H_2SO_4 in the fabric/dust cake structure. It should be pointed out that, although the loss of fabric strength can be associated with failed bags, it is not possible to reliably predict bag life on the basis of the residual Mullen Burst Strength of the fabric. Bags that had been in service for as much as ten years have been observed to remain functional even though they had lost a large fraction of their original Mullen Burst Strength. The end of bag life is determined by more variables than incorporated in the Mullen Burst Strength test.

Flue Gas Conditioning

Relevant insight has been gained in three studies in which flue gas conditioning was attempted on order to improve baghouse performance. Sulfur trioxide was injected as a conditioning agent, along with anhydrous ammonia, at one site while hydrated lime,

anhydrous ammonia, or a mix of the two were injected at two boilers burning high sulfur coal.

SO_3 Injection to Improve Dust Cake Cohesion, Porosity, and Particulate Collection Efficiency

A low-sulfur lignite coal produced fly ash with very low cohesion, very high pressure drop, and a propensity to penetrate fabrics such that opacity exceeded 20%.[32] In tests utilizing ammonia injection (25 ppmv), it was determined that particulate collection efficiency improved significantly (80% opacity reduction), while average drag experienced a moderate decrease (20%). In an attempt to attain still further reduction of pressure drop and emissions comparable to the baghouse design specification, ammonia injection was augmented with SO_3 injection (15 ppmv SO_3 with 31 ppmv ammonia) in a six month test. Pressure drop was reduced by 40% to 50% relative to a parallel baghouse without flue gas conditioning, and the emissions were effectively eliminated with combined SO_3 and ammonia.[33] Weights of conditioned bags became approximately 40% higher than bags without flue gas conditioning. Near the end of the trial, Mullen Burst Strength measurements were performed both on bags exposed to conditioned flue gas and on bags without conditioning. Both types of bags had been installed at the beginning of the trial. No significant difference in bag fabric strength was discerned.[33]

After the trial with combined ammonia and SO_3 conditioning ended, conditioning with ammonia continued using the same bags. Seven months later, large numbers of bags began to fail. Fabric strength measurements were then performed on another set of bags. Those that had not been exposed to conditioned flue gas exhibited Mullen Burst Strengths averaging 398 psig. The bags that had been conditioned with combined ammonia and SO_3 flue gas exhibited areas of differing strengths associated with an orange coloration on the clean side of bags. Areas without the coloration had average strengths of 374 psig whereas areas with coloration had average strengths of 147 psig.

The orange coloring was determined to be a manifestation of the deposition of elemental selenium. Selenium deposition was also observed at the two other sites where ammonia conditioning, described below, was used. An analysis of these dust cakes and these events yielded the following reaction as a probable mechanism to explain the collection of selenium on the bag surfaces:[34]

$$3SeO_2(g) + 4NH_3(g) = 3Se(s) + 2N_2 + 6H_2O(g)$$

Preservation of Fabric Strength When Exposed to Flue Gas from High Sulfur Coal

Two projects involved efforts to reduce the rate of reduction in bag strength associated with high-sulfur coal by injecting reactants to neutralize sulfuric acid, which had flue gas concentrations of about 10 ppmv at both sites. Injection of reactants eliminated SO_3 from the downstream flue gas in both investigations.

Compartment scale tests of ammonia injection lasting 24 months were performed at a full-scale baghouse controlling emissions from a boiler burning a high-sulfur, Eastern bituminous coal. Fabric strengths of bags from test compartments and a control compartment were performed after 6, 11, 13, and 25 months. Fabric strengths started at 640 psig at the beginning of the tests. Strengths of bag fabrics from the test compartments and a control compartment declined at the same rates through the first 13 months. However, at the end of 25 months, the strength of control bags averaged 180 psig while that of the test compartment averaged 70 psig.[28] Thus, in this instance, flue gas conditioning with ammonia did not reduce the rate of loss of bag strength but may have actually contributed to weakening of the fabric over the last 12 months of the investigation.

The other investigation of flue gas conditioning to neutralize sulfuric acid was part of a multi-year pilot scale project to characterize the performance of fabric filters in service with high-sulfur coal. Performance comparisons were carried among three compartments, one of which employed ammonia conditioning, the second employed conditioning with powdered hydrated lime, while the third treated unconditioned flue gas as a control. The feed rates of the reagents were set at stoichiometric ratios ranging from 2:1 to 10:1 relative to SO_3, but no variation of results were observed for ratios above 2:1.[31]

Flue gas conditioning with ammonia produced marked differences in the performance of the fabric filter. Ammonia conditioning altered the filtering characteristics of the dust cake to reduce pressure drop. The apparent mechanism for this effect was a reaction of ammonia with SO_3 to form an ammonium bisulfate/ammonium sulfate complex that increased the porosity of the dust cake as it was formed during the filtering cycle. However, the collected ash was more difficult to remove so that residual dust cake weight increased. In addition, the acidic ammonium bisulfate promoted acid attack to weaken the fabric as measured by its residual Mullen Burst Strength.

Conditioning with hydrated lime had little effect on pressure drop relative to the control compartment even though the residual dust cake weight was much lighter in the compartment conditioned with hydrated lime. Actually, pressure drop relative to the control

compartment was slightly higher.

Differences in post-exposure fabric strength, depicted in Figure 4, were attributed to differences in flue gas conditioning. In this figure, fabric strength retention is the ratio of Mullen Burst Strength at a given time to its initial value (at test initiation). Superior strength retention in the bags conditioned with hydrated lime suggested that removal of SO_3 protected the fabric from acid attack. Fabric strength in the compartment conditioned with ammonia deteriorated faster than in the control compartment.

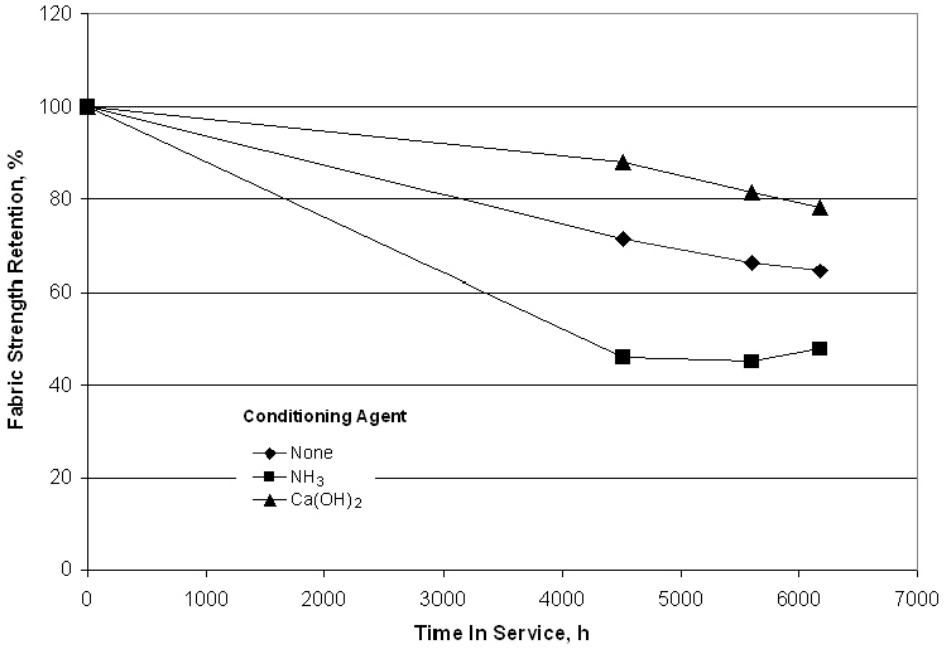

Figure 4. Fabric strength retention based on Mullen Burst Strength of the fabrics in compartments conditioned with anhydrous ammonia and hydrated lime.

Removal of SO_3

Without considering alkali injection or other flue gas conditioning to protect bags, Hardman and Dismukes[8] estimated the fraction of sulfuric acid removed from flue gas by baghouses to be 90%. Experiences such as those described above demonstrate that SO_3 and some SO_3 mitigation methods have a significant role in the performance of fabric filters in utility applications. The potential for heavy bags, low pressure drop, and reduced bag life associated with the presence of SO_3, are factors in the operation of a baghouse. Replacement bags are usually the most significant cost encountered in maintaining a baghouse. However,

conditioning with hydrated lime may dramatically reduce loss of bag strength and extend bag life. When this mitigation method is implemented, baghouse removal efficiency for SO_3 is essentially 100%.

SO_3 Effects on the Appearance of Stack Emissions

Although sulfuric acid in electrical power plant emissions has not been regulated directly, there has been motivation for many coal and oil-fired boilers to minimize SO_3 levels to avoid high visibility emissions. For those boilers with hot flue gas in the stack (i.e., without wet scrubbers), there are sometimes lower levels of opacity measured in the stack than in the plume above the stack. This increase in opacity, sometimes described as a "detached plume," is the result of acid vapor being converted to the particle phase resulting from flue gas cooling in the plume during mixing with ambient air. The purpose of the discussion to follow is to arrive at an estimate or range of the change in visible emissions for a given increase of sulfuric acid vapor.

Background

There are two features about visual observations of stack emissions that are relevant: attenuation of light passing through the plume as measured by opacity; and light scattered from all directions incident on the plume into the direction of the observer. When below 5% to 10%, opacity is difficult to measure accurately, but scattered light is still readily visible. Opacities well below 10% are common with modern, large particulate control technology, so the plume appearance is dominated by scattered light. Therefore, this discussion focuses on scattered light although the measure of it is the same as addressed in opacity concerns. Light absorption by coal-fired boiler ash is rarely significant, so scattering is the cause of opacity.

The scattering coefficient, γ, of flue gas or a plume exiting the stack represents the total effective particle light-scattering cross sectional area per unit of path length. When the depth or thickness (L) of the flue gas or plume is small enough such that $\gamma L < 0.2$, the intensity of scattered light is directly proportion to γL. Opacity (Op) is related to the scattering coefficient by $Op = 1 - T = 1 - e^{-\gamma L}$ where T is transmittance, the fraction of a light beam not scattered. Note that opacity is also given by γL when $\gamma L < 0.2$. While light scattering varies dramatically with particle size, the scattering coefficient characterizes the net combined effects of scattering variation with size and the distribution of particle sizes for a particular sample. The magnitude of scattering by a particle is expressed in this discussion in terms of ratio of the particle's effective cross sectional area to its volume. This ratio is called the specific scattering coefficient, γ^*, and has units of reciprocal length. If particle size is

expressed in micrometers, γ* has units of inverse-micrometers ($\mu m^2/\mu m^3$, or μm^{-1}). A plot of γ* versus particle diameter is shown in Figure 5. The differential scattering coefficient, dγ/dLogD, is the product of γ* and the distribution of particulate loading of the effluent with particle size on a volume basis, dV/dLogD. It is convenient to express dV/dLogD in units of cubic centimeters per cubic meter (cm^3/m^3) and γ* in reciprocal micrometers (μm^{-1})so that the resulting unit of the product without further conversion is in units of reciprocal meters (m^{-1}), the unit normally employed for scattering coefficient, γ. Consideration of the differential scattering coefficient is useful to characterize the relative contributions of the aerosol size components to the overall scattering coefficient. Figure 5 shows dγ/dLogD for the example ESP outlet particulate loading and size distribution of Figure 2 (dM/dLogD, particle density of 2.35 g/cm^3). In this example, about half of the total γ would derive from particles around 1 μm, and the larger sizes, the bulk of the particulate volume (or mass), would contribute the other half. Note that dividing γ by V, the total particulate volume concentration, results in the average of γ* over size, weighting it by the normalized particulate volume size distribution. For the example, V is 0.026 cm^3/m^3, so γ/V is 0.77 m^2/cm^3.

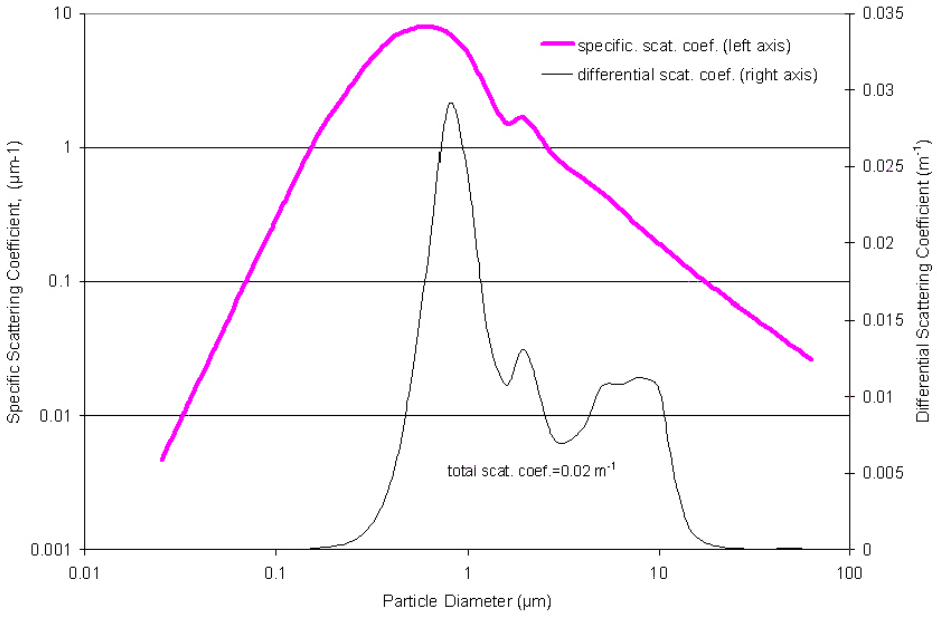

Figure 5. Specific light scattering coefficient per particle volume (left axis) and contributions of the outlet particulate matter of Figure 2 (right axis).

When acid vapor is converted to particulate phase, heterogeneous condensation onto preexisting particles takes place as a diffusion limited process. Acid is condensed in proportion to particle diameter for particles larger than the gas mean free path (about 0.08 μm) and proportional to particle area for those smaller than the mean free path.[35] Dependence on particle diameter means that the heterogeneous condensation rate across the particle size spectrum is weighted toward fine and ultrafine particles relative to the particle mass distribution. If cooling of the vapor is fast then the equilibrium vapor pressure of the acid can decline much faster than actual vapor pressure due to limitation by diffusion to available particle surfaces. Then supersaturation becomes high enough to result in homogeneous nucleation at the molecular level. The very large number of particles produced in the nucleation process rapidly grows by coagulation. The number concentration of particles in this mode is very much larger than the number concentration of the preexisting particles. For example nucleation of 10 ppmv of H_2SO_4 produces particle number concentrations on the order of 10^{16} per cubic meter when their size has grown to approximately 0.05 μm, while the total number concentration of preexisting particles is on the order of 5×10^{11} per cubic meter.[36] In such cases, coagulation is characterized as self-preserving, dominated by self coagulation, in which the mode grows with the mean size increasing while the width of the mode is constant[35] (1.32 geometric standard deviation[37]). Self coagulation (i.e., between particles within this mode formed by nucleation) dominates as opposed to coagulation with preexisting particles because of the dominance in particle number in this mode. Of course, particles in this nucleation mode also provide surface area for homogenous condensation in competition with heterogeneous condensation on preexisting particles. This example suggests that nucleation deposits more acid in ultrafine particle sizes (less than 0.2 μm) than occurs by heterogeneous condensation, depending upon the magnitude of the ultrafine mode of the fly ash. In view of the large variation of specific scattering coefficient with particle size as shown in Figure 5, it is obvious that the impact of sulfuric acid vapor on the appearance of stack emissions depends substantially on the fraction nucleated versus the fraction condensed to preexisting particles. Within the latter, the weighting of condensation rates as a function of particle size is important, resulting in relatively lower scattering if condensation is to sizes smaller than 0.2 or larger than 2 μm.

Field Observation of Nucleation

Detailed measurements of plume characteristics near a stack are impractical. Therefore, plume simulation hardware and procedures were developed for surrogate measurement.[38,39] A specific example that appears informative was obtained by this method during a field test at a coal-fired boiler.[38,40] Figure 6 gives particle size distribution and mass of the aerosol in a

coal-fired boiler stack, measured with cascade impactors, along with that in the "plume" formed in the air-dilution plume simulator measured with an electrical mobility aerosol analyzer. For dilution and cooling in the plume simulator, flue gas was extracted from the stack through a fine particle separator, maintained hot, and injected vertically upward at the bottom-center of a vertical, 8-inch-diameter mixing-chamber with concentric ambient air dilution flow. The hardware was designed to provide a residence/mixing time of 10 seconds with a dilution ratio of 20:1. The large increase from stack gas to plume simulator in the number of particles at sizes smaller than 0.1 μm (see Figure 6) is indicative of a strong component formed by nucleation and coagulation. A particulate mass concentration of 2 mg/dncm in the stack for particles smaller than 2 μm became 41 mg/dncm in the "plume" through some combination of condensation and homogeneous nucleation. The given "plume" values are relative to stack conditions, before dilution, corrected to dry normal conditions (1 atm., 20 °C). The measured total loading is consistent with the measured 6.5 ppmv SO_3 by the controlled condensation reference method in the stack with 30% combined water.

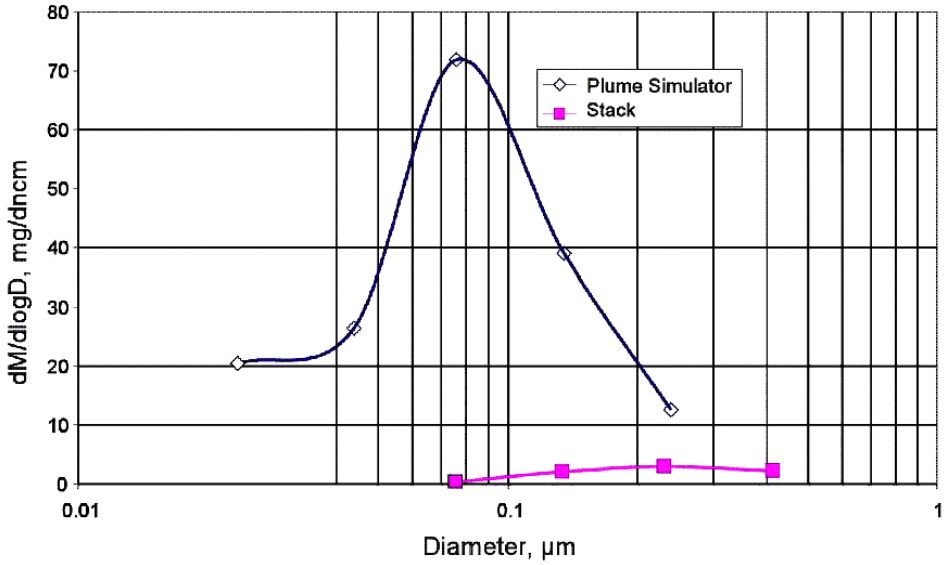

Figure 6. Measured particle mass versus size in stack and in "plume" formed in plume simulator. (Sample from a coal-fired boiler ESP exit at 300 °F with 6.5 ppmv of H_2SO_4 vapor was diluted so as to realistically simulate a near-stack plume.)

There was no visible stack plume during the tests in which these data were obtained. Consideration of plume appearance or light scattering (in terms of γL) leads to consideration of plume concentrations, dilution, and thickness during observations. As flue gas exits the

stack, it spreads and slows in velocity as well as being diluted and cooled. The spreading, slowing, and cooling contribute to an increase of path length, L, which tends to compensate the decrease in γ caused by dilution. DeFries[41] investigated the degree of compensation for conditions of no gas to particle conversion and concluded that use of stack or undiluted concentrations and stack diameter to be adequate for estimating plume values of γL (less than 16% positive error). Note that the dilution process slows the process of particle growth by coagulation. The calculated scattering coefficient for the plume, including liquid-phase acid (acid droplet density of 1.6 gm/cm^3), as depicted in Figure 6 in this example, was 0.006 m^{-1}. This result includes 0.0003 m^{-1} contributed by coarse particles totaling 22.5 mg/dncm (ash density of 2.35 gm/cm^3) that were separated from the flue gas passed to the plume simulator but were in the actual plume. For a stack diameter of 5 m, the calculated scattering produced an opacity of 3%, a low value consistent with no visible plume. This contribution to scattering coefficient by the nucleated acid in this example was 0.004 m^{-1} for 6.5 ppmv acid, or 0.22 μm^{-1} for the average γ*, the specific scattering coefficient of the acid droplets for this case.

Survey of Scattering Coefficients for Stack Plumes

A comprehensive theoretical model of particulate matter formation in emission plumes has been developed (Damle, Ensor, and Sparks[42]) that provides qualitative agreement with observations. Unfortunately, field data for validation purposes are unavailable in which SO_3, visible emissions, particulate size distribution, temperatures, flow rates, and moisture are quantified simultaneously. Even so, this model is considered useful as a survey tool. Results have been reported using the model to predict the effects of changes in acid vapor concentration. Other parameters varied were fine particle concentration, coarse particle concentration, water vapor, plume temperature, wind speed, and ambient humidity and temperature.[41,43] In one series of comparisons, baseline conditions were defined that included 100 mg/m^3 of coarse particles, 10 mg/m^3 of fine particles, 10 ppmv of sulfuric acid vapor, and reasonable values of 6 other stack parameters, 5 other ambient parameters, and geometric standard deviations of the 2 preexisting particle size modes. The geometric mean size of these two modes were 0.15 and 4 μm on particle number basis, or 0.33 and 10 μm on mass basis, for the fine and coarse modes, respectively. For the baseline conditions, the increase in the average specific scattering coefficient, γ^*_{ave}, resulting from condensed acid was 2.5 μm^{-1}, indicating heterogeneous condensation contributed significantly in the 0.5 to 2 μm range. Other parameters were varied individually and resulted in little change in γ^*_{ave} except in the cases of reducing the fine particle loading to 1 mg/dncm and increasing wind speed to 20 m/s from 5 m/s. In both of these cases, the increase in γ^*_{ave} was reduced to 0.67 μm^{-1} (from 2.5 μm $^{-1}$). In the first instance, less heterogeneous condensation to the fine

mode was probably the reason for a smaller increase in γ^*_{ave}. In the second instance, increased nucleation is suspected. Another series of calculations was performed with the fine mode loading reduced to 2 mg/dncm and varying acid vapor from 10 to 40 ppmv. In each of these instances, the increases in γ^*_{ave} were only around 1.2 μm^{-1} (from 2.5 μm^{-1} in the base case). Decreasing the fine particle loading to zero and varying acid vapor between 10 and 40 ppmv produced increases in γ^*_{ave} of 0.2 μm^{-1} at 10 ppmv sulfuric acid, 0.3 μm^{-1} at 30 ppmv, and 0.62 μm^{-1} at 40 ppmv. This increase in γ^*_{ave} with increasing acid vapor was necessarily the result of predicted nucleation. Another test case assigned 2 and 10 mg/dncm to the fine and coarse modes and produced a predicted increase in the scattering coefficient per volume of acid of 0.6 μm^{-1}.

A correlation seems to exist concerning the increase in γ^*_{ave} due to condensed sulfuric acid vapor in stack plumes and the original concentration of fine particles in the stack. The apparent range of expected values of γ^*_{ave} is an order of magnitude, 0.2 to 2.5 m^{-1}, but where a specific site lies within that range is determined primarily by the loading of in-stack fine particles. In general, lower fine particle loadings cause lower values within that range of increase in the scattering coefficient, presumably due to increased nucleation. A high fine particle in-stack loading is 10 mg/dncm, and a low value is 2 mg/dncm. High coarse particle loadings limit values of the increase in scattering coefficient per unit volume in the upper part of the range. Coarse particle loadings are generally negligible when fine particle loadings are low because control strategies for fine particles tend to incidentally control coarse particles very well.

An Indicator of Particle Size Characteristics in Stack Plumes

The appearances of stack plumes are frequently reported as blue in color. This effect is the result of scattering of blue light by particles less than 0.3 μm being dominant over scattering at other wavelengths. This blue tint indicates an unusually high concentration of these particles relative to larger sizes. The specific scattering coefficient in Figure 5 is the spectral average weighted by the photopic response from 420 to 650 nm. In this particle size region (size much, much less than wavelength), scattering is inversely proportional to the fourth power of wavelength, so the scattering by each of these particles for blue light is significantly higher than that for the longer wavelengths. That is, this strong dependence on wavelength in this region below 0.3 μm causes scattering to be stronger for blue light. Scattering by particles of a broad size distribution greater than 0.5 μm is about the same for all colors of the visible spectrum. For this blue tint to be apparent, scattering by the larger particle size fraction must be small. This same dependence of scattering on particle size and wavelength causes light transmitted (that not scattered) to have a brown color; that is,

depleted in blue light. There is a relevant exception to this scattering phenomenon for the correct interpretation of brown color that is associated with light absorption by NO_2. Nitrogen dioxide gas concentrations are sometimes high enough to absorb blue light, causing the transmitted light to have a brown color. This absorption has no relation to particle scattering; so when blue scattered light is observed, one can be confident of ultrafine particles being present in significant concentrations.

4. NO_X Reduction Catalysts (SCR)

Production of SO_3, Relationships with Catalysts and Other SCR Parameters

SCR technology has been developed with foreknowledge of the fact that catalytic oxidation of SO_2 to SO_3 accompanies NO_X reduction when this technology is employed, at least with current vanadium-based SCR catalysts. Thus, the potential for problems related to SO_3 production has been recognized throughout the history of SCR development. Nonetheless, it has become the most widely used NO_X control system. In Japan and Europe, early commercial installations in the 1980s experienced SO_2 conversion rates of 1% to 2%, whereas current domestic installations typically have conversion rates on the order of 1% or less. The higher conversion rates of the early foreign installations were mainly due to the lower sulfur contents often present in the foreign fuels as compared with domestic fuels and to the relatively early nature of the catalyst design (catalysts have been optimized significantly to minimize SO_2 conversion since these early installations). Figure 7 gives results of an investigation related to SCR with high sulfur coal that was performed as part of a DOE Clean Coal Project examining SCR applied to high sulfur coals.[45] As seen in the upper graph (a), there was a large variation of oxidation rate from catalyst to catalyst produced by different manufacturers. The investigators concluded that this resulted from different choices by each manufacturer involving tradeoffs with other parameters such as catalyst volume, pressure drop, ammonia slip margin, and overall design margin. The project specifications required that the SO_2 oxidation rate be less than 0.75% at 700 °F for all catalysts submitted for the test program. All catalysts satisfied that limit, and it was concluded that any of the manufacturers could attain lower values of oxidation rate by increasing catalyst volume (and capital cost) as a result of formulation changes. Catalyst volume could be held constant while lowering SO_2 conversion, but physical changes would be required which would effectively increase total catalyst surface area present at the expense of pressure drop. These trade-offs occur because a lowering of the SO_2 conversion rate requires that the catalyst be less active on a specific geometric surface area basis. This lower activity must then be offset by increased catalyst volume or by a more dense catalyst geometry that would produce higher pressure drops.

Many operating factors influence SO_2 conversion to SO_3 in an SCR, including reactor temperature, flow rate, and SO_2 levels. The SO_3 conversion rate of an SCR is normally measured by simultaneous sampling from its inlet and outlet ducts using a manual procedure, the controlled condensation method described in a later section. The SO_3 results are expressed in terms of percent SO_2 oxidation. In most cases, SO_2 conversion is linearly

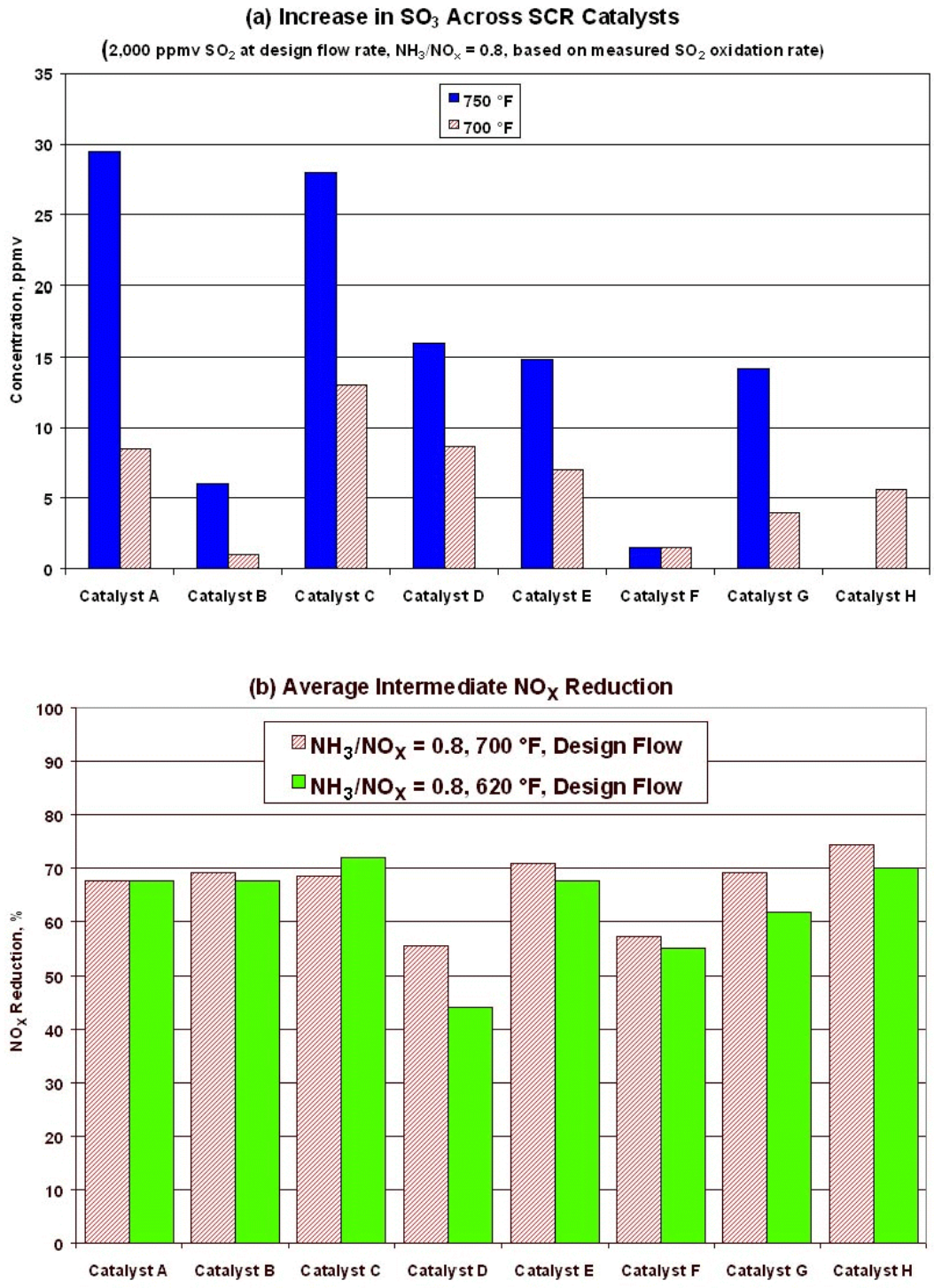

Figure 7. Oxidation of SO_2 to SO_3 (a) for several SCR catalysts at 700 and 750 °F and corresponding NO_X reduction (b) at 700 and 620 °F from a pilot scale investigation at a coal-fired utility boiler burning 3%-sulfur coal.[45]

and inversely proportional to reactor flow rate, and relatively independent of absolute SO_2 concentration. With respect to temperature, however, the change in conversion rate is more exponential, making temperature the most critical operating parameter affecting SO_2 conversion. Consequently, conversion may increase dramatically above the normal design temperature range for a particular installation.

Figure 7(a) clearly shows the strong relationship of SO_2 conversion to temperature. The exact nature of the relationship depends on many factors including catalyst formulation and the specific nature of the field application. However, SO_2 conversion will always decrease with temperature when other factors are held constant. NO_X reduction ($deNO_X$) capability will generally decrease with temperature as well. This decrease is illustrated in Figure 7(b). Note that the figure presents NO_X reduction for a single catalyst layer at a constant NH_3/NO_X ratio. A relatively small change in single-layer $deNO_X$ level is multiplied across layers and, therefore, results in a larger decrease in $deNO_X$ capability for the installation as a whole. Thus, for most catalysts, the ability to reduce NO_X (assuming slip must be held constant) is strongly impacted by a reduction in operating temperature. In practice, the benefits of lowering the operating temperature for a particular installation (to lower SO_2 conversion, for instance) are offset by increased catalyst volume required to maintain desired $deNO_X$ capability, assuming the catalyst formulation is not changed. While it may be possible to minimize temperature impacts on $deNO_X$ capability in order to minimize SO_3 formation, the impacts on total plant performance are most often adverse and must be taken into account. Thus, no net positive effect is typically gained by lowering operating temperature strictly as a means of SO_3 control. Optimally, the typical operating conditions for a facility are well known and are considered during the specification of the catalyst and the resulting formulation that is used. The maximum SO_2 conversion rate is a specified parameter, along with $deNO_X$ capability, and in practice, most requirements can be met by the catalyst suppliers. Tight SO_2 conversion specifications will result in increased catalyst volume, increased pressure drop across the catalysts, or both. Thus, an overly constraining SO_2 conversion requirement would result in unnecessary increased facility capital and operating costs. The difficulty in specifying the allowable SO_2 conversion is exacerbated by the poor understanding of the behavior of SO_3 downstream of the boiler and upon release at the stack.

The need to apply SCR to a wider variety of fuels with highly variable characteristics has dictated that catalyst designers meet ever widening design criteria.[44] In addition, end-users are requiring more flexibility in SCR operating characteristics to match unit-specific circumstances, which contributes to the range of SO_2 oxidation rates and resulting SO_3

levels being offered by catalyst manufacturers. SCR specialists expect that the capabilities of SCR catalysts will continue to expand as additional research and development is fueled by increased use of the technology.

For large coal-fired utility boilers within the United States, the most common SO_2 oxidation specification is 1%. However, facilities firing high sulfur coal or facilities known to have high rates of combustion-related SO_2 conversion may opt for lower conversion rates, as low as 0.5%. Alternately, units firing very low sulfur coal, such as Powder River Basin coals, may opt for higher conversion rates, on the order of 1.5%, or possibly more. Cost savings accompany higher conversion rates. The trend in domestic plants has been a lowering of the specified SO_2 conversion. The actual rate of SO_2 conversion will vary over time as discussed subsequently. Thus, specifications for SO_2 conversion must consider the long-term oxidation rates, not just the initial expected conversion.

Ammonia Slip

Ammonia slip refers to the small amount of ammonia that passes unreacted through the SCR catalyst. Ammonia slip is a function of catalyst formulation, volume, age, and specific operating conditions. As such, it is a specified parameter in both design and operation. Even a poorly operating SCR system can typically achieve required NO_X reduction levels, but at the expense of higher ammonia injection rates and increased ammonia slip.

Most coal-fired facilities specify ammonia slip to be held to less than 2 ppmv over the life of the installation and across the normal operating range for the facility while achieving the required NO_X reduction. Slip levels as much as 5 ppmv in coal-fired facilities are often manageable from an operational standpoint, but concerns over fly ash contamination typically require that slip be held to lower levels. Usually, the SCR is located upstream of the particulate control device. In practice, ammonia slip is often higher than that predicted by the design criteria for the facility. This is due to the inability to easily measure and track ammonia slip, which, in turn, means that injection rates tend to be set with some margin over what is believed to be the minimum needed for the required NO_X reduction. From this standpoint, actual field measured slip levels are likely to be higher than would be indicated by the facility design criteria discussed previously, ammonia in the presence of SO_3 was also associated with fabric strength problems in baghouse operation. The ammonia levels of those investigations were an order of magnitude higher than ammonia limitations associated with fly ash contamination related to ash byproduct utilization. More restrictive limitation of ammonia slip is necessary in order to permit use of fly ash as a byproduct rather than disposal as solid waste. Therefore, current SCR design typically provides for lower slip than

in earlier installations while maintaining the NO_X reduction required by the utility system's NO_X compliance strategy. Equipment downstream of the air preheater may also be affected by ammonia byproduct formation. In this regard, SCR impacts on particulate control devices such as ESPs and baghouses are discussed below.

Variation of SO_3 Production and Ammonia Slip Over Catalyst Life

The levels of SO_3 and ammonia slip will vary over time for a particular SCR installation. This occurs primarily as a result of catalyst deactivation and catalyst management activities discussed below. Ammonia slip will gradually increase as the catalyst deactivates and ammonia injection is increased to maintain the necessary NO_X reduction. A level of ammonia slip is specified at which catalyst addition or a partial catalyst replacement is necessary. It is at this point in time that the catalyst "end-of-life" has been reached, although a great deal of NO_X reduction activity is still present. This end-of-life is consequently a specified condition—the point at which ammonia slip reaches some predetermined value. Thus, a guaranteed maximum slip value of 2 ppmv requires that the ammonia slip not exceed 2 ppmv at the catalyst end-of-life. Consequently, the average ammonia slip for a particular catalyst charge over its life will be lower than the guaranteed level, averaging roughly 1 ppmv for a unit with a 2 ppmv slip guarantee (assuming a linear deactivation rate). Most SCR reactors are constructed with space for one or more spare layers of catalyst. The most frequent design is a three-layer system where two layers are installed initially, and a third layer is installed at the end-of-life of the initial charge. This produces a step change in activity, carrying the reactor forward in time for several additional years of service. Thereafter, replacement of catalyst beds will occur, again producing step changes in activity. Initial catalyst lives are typically on the order of 16,000 to 24,000 operational hours, depending on the specific unit. Catalyst additions or partial replacements will usually extend the operating life by 16,000 hours or more.

SO_2 conversion to SO_3 does not decline over time as would be indicated by the decline in NO_X reduction activity for a particular charge of catalyst.[46] This is somewhat counterintuitive and is due to the nature of the catalyst with respect to active sites as well as mass transfer contributions. As a result, a particular charge of catalyst will exhibit a near constant SO_2 oxidation rate over its entire life in the reactor and at a particular operating condition. Only when additional catalyst is added will a step change in SO_2 conversion be noted. Consequently, assuming that all catalyst formulations are identical, SO_2 conversion will be a function of total installed catalyst volume only, irrespective of the age of the catalyst present. For example, an SCR system having a two-bed initial catalyst charge that has a 1% SO_2 conversion rate will experience a 50% increase in SO_2 conversion with the

addition of the third catalyst bed, resulting in a SO_2 conversion rate of 1.5%. This conversion rate will then be constant over the remaining life of the installation irrespective of catalyst replacements (assuming that all catalyst formulations are identical and the total catalyst volume remains constant). Thus, most facilities will experience one step-change in SO_2 conversion, which occurs at the installation of the spare layer of catalyst, and conversion remains constant thereafter, assuming that three layers continue to be utilized. This conclusion is based on the expectation that catalyst management will proceed without replacing two of the layers and removing a third one.

Options for Controlling Ammonia and SO_3

Assuming that it is well distributed, the amount of ammonia absorbed on the catalyst is proportional to the ammonia injection rate, and this determines the NO_X reduction. Ammonia slip is also proportional to injection rate. Normal operation of SCR is predicated on the requirement that a specified NO_X reduction is achieved by increasing ammonia injection as needed. In many systems, this is achieved by direct control of ammonia injection based on continuous NO_X monitors. Consequently, ammonia slip is not controlled by limiting injection but can only be controlled through the design of the SCR facility, its catalyst, and its optimization to attain a desired level of slip resulting from the condition that the required NO_X reduction is maintained. Facility design issues such as reactor inlet flue gas distributions (ammonia, flow, temperature, NO_X) will influence the performance of the SCR reactor and the resulting ammonia slip. Catalyst design will of course help to minimize slip, with formulation and volume being related to the desired slip levels and SO_3 production levels. Once the facility is installed, optimization procedures to tune the system will aid in the reduction of ammonia slip.

When the particulate control is at the cold side of the air preheater, SO_3 may enhance removal of ammonia through the formation of sulfates of ammonia that can be collected by an ESP or baghouse. When dealing with coals for which SO_3 formation is very low, it may be desirable to design the SCR for enough SO_2 to SO_3 conversion to assure reaction with ammonia slip. The presence of reactants other than SO_3 and the degree of adsorption of ammonia by fly ash has not been addressed.

There may be a need to limit SO_3 depending on alkali, alkaline earth, and sulfur content of the coal to avoid corrosion or reduce the visibility of emissions as described above. Concerning control of SO_3, similar options are available related to the SCR facility itself, mainly centering on the catalyst formulation and volume. Since SO_2 is evenly distributed, temperature is the only distribution parameter that significantly effects SO_3 production from

the SCR. Maintaining the design temperature for the SCR is important.

Options for controlling SO_3 elsewhere in the boiler effluent, such as injection of alkali downstream of the SCR or air preheater, are available. However, the costs of the auxiliary control schemes should be weighed against the cost of controlling SO_3 via SCR design. In practice, for facilities that have identified a need to control SO_3 production from the SCR (lower than the 1% rate for most SCRs), catalyst formulation changes and volume increases are typically preferable compared to alkali injection. This is primarily due to the comparative capital costs of the two options, as well as the long-term operating costs and attendant operating difficulties of alkali injection systems. Alkali injection requires an additional plant system, transport and storage of alkali material, and manpower to maintain the injection system versus the static system associated with the catalyst control option.

As a comparative example of alkali injection costs versus the costs associated with a low-SO_3 production catalyst, a 500 MW unit burning 2.6% sulfur coal is referenced (based on a study at EPRI's High Sulfur Test Center).[47] For this facility, it was estimated that a limestone injection system using purchased limestone on the open market would cost approximately $500,000 a year on a 15-year levelized basis. Comparatively, it is estimated that for a similar facility operating at 90% NO_X reduction levels and using a 25% catalyst volume incremental increase, the additional cost for controlling SO_3 production from 1% to 0.5% would be approximately $230,000 a year on a levelized basis (based on a 24,000 hour life, catalyst cost of $5,500 per cubic meter, and an initial charge of 500 cubic meters for the 1% conversion option). Catalyst-based control options are often attractive if the required SO_3 control is within reach via catalyst modifications. Other factors will, of course, play a role in the decision and, consequently, the technical and economic issues are highly site-specific. However, to date, most facilities have opted for catalyst based SO_3 control rather than alkali injection, assuming that proper consideration is given prior to the installation of the SCR facility. In situations where problems are encountered after the installation of the SCR system, alkali injection for control is one of the few options available, since a reduction in the SO_3 produced by the catalyst would require a replacement of the entire charge of catalyst. Obviously, the desired final levels of absolute SO_3 are also important—SO_3 control using catalyst modification is, of course, very limited in magnitude compared to what could be achieved with alkali injection.

Ammonium Sulfate and Bisulfate Aerosol

It is well known that ammonia and SO_3 produced in SCRs react to form ammonium sulfate or bisulfate and some of it is deposited on internal surfaces of the air preheater. This

deposition is reflected by gradual increases in flue gas pressure drop across the air preheater with installation of SCR. The increased pressure drop is managed by soot blowing. Characteristics of the products of this reaction are of interest because of relevance to air preheater operation and to PCD operation downstream of air preheaters. Observations concerning ammonia injection upstream of a baghouse are discussed above. Previous observations concerning ammonia injection upstream of ESPs found that collection efficiency was enhanced in some instances.[4]

To explore possible behavior of the ammonia/SO_3 system, it is useful to make some approximate calculations of reaction regimes and aerosol formation. Under the conditions of temperature at which ammonium sulfates are observed to form, SO_3 will have reacted with water vapor to form sulfuric acid vapor; therefore, the reactants in the cases of greatest interest are ammonia and sulfuric acid. Although the thermodynamically favored product of the reaction is ammonium sulfate, the initial product is observed to be ammonium bisulfate. Ammonium sulfate is formed only after longer periods of time in the presence of excess ammonia. The melting temperature of ammonium bisulfate is 146.9 °C (296.4 °F), below the temperature at which, as shown below, it typically begins to form in flue gas. Therefore, the initial product is liquid. The reaction forming ammonium bisulfate is then:

$$NH_3(gas) + H_2SO_4(gas) = NH_4HSO_4 \text{ (liquid)}$$

An equilibrium constant of 1 for this reaction was calculated from thermodynamic data by Burke and Johnson.[48] Consider ammonia and SO_3 concentrations at the low end of the ranges discussed in Section 3 (e.g., 2 ppmv of NH_3 and 10 ppmv H_2SO_4 leaving the SCR). At these levels, according to Burke and Johnson,[48] ammonium bisulfate formation is not expected until the gas has been cooled to 160 °C (320 °F). At the other end of the range of possible concentrations, 5 ppmv NH_3 and 40 ppmv H_2SO_4, the onset of ammonium bisulfate formation is expected at 176 °C (349 °F). At a typical air preheater outlet temperature, say 150 °C (302 °F), the equilibrium constant is equivalent to 4.7 ppmv,[2] so control of ammonia slip and acid formation at low levels of, for example, 0.5 ppmv NH_3 and 9 ppmv H_2SO_4 would be required to completely avoid ammonium bisulfate formation inside the air preheater.

In an air preheater channel on the flue gas side, the temperatures of both wall and gas decrease in the direction of gas flow. The lowest gas temperatures at a given axial position are those adjacent to the wall. Formation and condensation of ammonium bisulfate, therefore, occurs first at the wall at the location where the metal temperature reaches the

critical value according to the equilibrium constant. Starting at this axial position, a boundary layer forms in the gas at the wall, within which there is a gradient in ammonium bisulfate concentration and where the temperature is equal to, or below, the critical value for ammonium bisulfate nucleation and condensation. The reaction front where ammonia and sulfuric acid form ultrafine droplets of ammonium bisulfate is the surface where this boundary layer meets the free stream. The resulting droplets travel toward the wall by diffusion and thermophoresis, driven by the concentration and temperature gradients, respectively. If the critical temperature for ammonium bisulfate formation is reached far enough from the outlet of the air preheater, the ammonia-sulfuric acid reaction front eventually propagates to the center of the channel, forming ultrafine droplets over the entire cross section of the flow.

Continuing in the direction of the flow, the following processes occur simultaneously as the gas cools: (1) formation of new nuclei and condensation of additional ammonium bisulfate on existing droplets, (2) growth of the droplets by coagulation, (3) deposition of droplets on the wall of the channel, (4) agglomeration of the droplets with fly ash particles, and (5) removal of ammonium bisulfate deposits from the wall by collisions of fly ash particles. As a result of these transformations, ammonium bisulfate can leave the air preheater in any of the following forms: (1) as ultrafine droplets or particles, (2) on the surface of fly ash, (3) as particles produced by erosion of deposits by fly ash, (4) as coarse particles produced during soot blowing of the air preheater, and (5) as particles reentrained into the combustion air when the flow direction in the air preheater channel reverses.

Estimates of the distributions of ammonium bisulfate over ultrafine particles, fly ash, and the air preheater surface and its contribution to ultrafine particles entering the particulate control device were found by a calculation of the behavior of ammonium bisulfate during its formation in a cylindrical channel and its evolution during the time it would take to travel from the air preheater to the particulate control device. The acid and ammonia levels were chosen toward the upper end of the ranges of conditions expected in coal-fired boilers, as discussed elsewhere in this report. The most important of the processes described above were included in the calculation:

1. Reaction between sulfuric acid and ammonia to form ammonium bisulfate condensation nuclei.
2. Growth of the liquid ammonium bisulfate droplets by coagulation.
3. Agglomeration of ammonium bisulfate droplets with fly ash.
4. Deposition of ammonium bisulfate on air preheater surfaces by diffusion and thermophoresis.

The assumed conditions were as follows:

Initial sulfuric acid: 40 ppmv
Initial ammonia: 5 ppmv
Temperature gradient in the air preheater: 128 °C/m (70 °F/ft)
Temperature leaving the air preheater: 150 °C (302 °F)
Temperature difference, flue gas to metal: 55.6 °C (100 °F)
Gas velocity: 14.6 m/s (48 ft/s) (constant)
Diameter of air preheater passages: 10 mm
Residence time between air preheater and particulate control device: 5 s

At the initial ammonia and acid concentrations chosen for the calculation, the equilibrium constant of Burke and Johnson[48] predicts the onset of ammonium bisulfate nucleation at 176 °C (349 °F) and 0.205 m (8 inches) from the exit of the air preheater. Because of the strong interaction between ammonia and sulfuric acid, the rate of formation of ammonium bisulfate was estimated to be the frequency of tri-molecular collisions between ammonia, sulfuric acid, and any other gas molecule. The size of the critical nucleus was taken equal to the size of a single ammonium bisulfate molecule, consistent with the assumption that all tri-molecular collisions that include an ammonia and a sulfuric acid molecule result in formation of product. Growth of the droplets by coagulation was estimated using the expression of Friedlander[35] for growth of a self-preserving particle size distribution. This is an approximation, since the distribution is not exactly self-preserving in the presence of continuous nucleation and condensation as the gas cools. However, the cooling rate and corresponding rate of production of ammonium bisulfate are slow.

The rate of agglomeration of the droplets with fly ash was found from the standard description for mass transfer of nanoparticles to larger suspended particles, using the diffusion coefficient for the local mean size of the ammonium bisulfate droplets. Because the size distribution of the fly ash was broad and bimodal, it was divided into two parts having characteristic sizes of 0.09 and 7 μm and external surface areas of 0.1 and 3 square meters per cubic meter of flue gas (at 25 °C and 1 atm). Approximately twice as much ammonium bisulfate is collected on the smaller fly ash particles, compared to that collected on the larger particles.

The Reynolds number of the flow in the air preheater channels under the conditions chosen is 5000. Deposition of ammonium bisulfate on the air preheater surface was treated using standard relations for mass transfer in turbulent flow, with the Schmidt number for the ultrafine particles determined using the diffusion coefficient for the local mean size of the

particles.

The assumed temperature gradient in the gas in the air preheater is shown in Figure 8a. The calculated distribution of ammonium bisulfate among ultrafine particles, fly ash, and air preheater surface is shown in Figure 8b and the corresponding droplet sizes in Figure 8c. All are shown as functions of distance along the 10-mm diameter air preheater channel. The residence time in the length of channel shown (8 inches) is 0.014 seconds. Under the assumption that its rate is limited by the frequency of tri-molecular collisions, the reaction forming ammonium bisulfate is very rapid with respect to the cooling rate; therefore, the incremental amount of ammonium bisulfate formed in any time or distance interval is given, to good approximation, simply by the change in the equilibrium constant associated with the drop in temperature. This process determines the rise in concentration of ultrafine droplets shown by the dashed curve in Figure 8b. Transport of droplets to the surfaces of fly ash particles and the wall of the channel are relatively slow, removing only small fractions of the ammonium bisulfate droplets from the gas as shown by the solid and dashed curves near the bottom of Figure 8b. At 150 °C (302 °F) (the temperature of flue gas leaving the air preheater), 4.9 ppmv of ammonium bisulfate has formed, and 4.9 ppmv of each of the reactants has been consumed, leaving only 0.1 ppmv of ammonia and approximately 35 ppmv of sulfuric acid unreacted. Approximately 2.5% of the ammonium bisulfate formed is estimated to have deposited on the fly ash, 4% has deposited in the air preheater, and 93.5% remains suspended as ultrafine droplets in the flue gas. Because the amount of condensing material and residence time are both small, the calculated mean droplet size leaving the air preheater is only 0.0046 μm, as shown in Figure 8c.

The evolution of this system over 5 s at the same temperature at which it left the air pre-heater (150 °C, 302 °F) and in the absence of any additional loss of particles to heat transfer surface or walls is shown in Figure 9. The processes occurring in the air preheater are also shown, but they now appear compressed into a very small fraction of the time scale (the first 0.014 s) on the left side of the figure. Under the present set of approximations, no additional ammonium bisulfate forms during passage from the air preheater to the particulate control device because the temperature is fixed. The only processes that occur are growth of the ultrafine droplets and particles by coagulation and collection of the ultrafine droplets and particles by fly ash. At the entrance to the particulate control device, 4.1 ppmv of ammonium bisulfate are estimated to be present as ultrafine droplets or particles suspended in the flue gas, 0.6 ppmv are combined with the fly ash, and 0.2 ppmv were left behind in the air preheater to be reentrained as large agglomerates during soot blowing. The mean size of the ultrafine particles has grown to approximately 0.06 μm by this time.

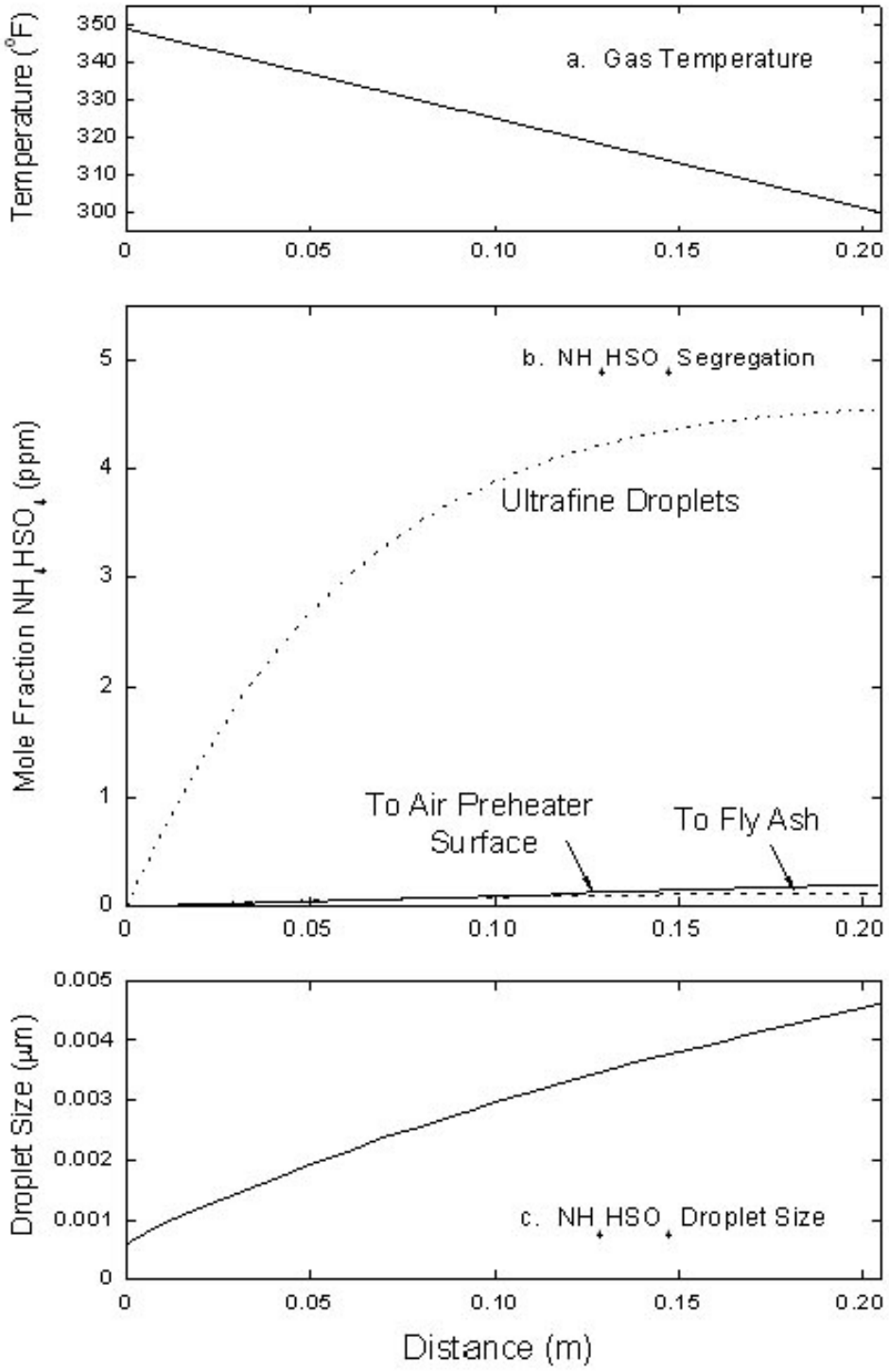

Figure 8. Distribution of ammonium bisulfate among ultrafine particles, fly ash, and air preheater surface and corresponding droplet sizes versus distance along the channel wall.

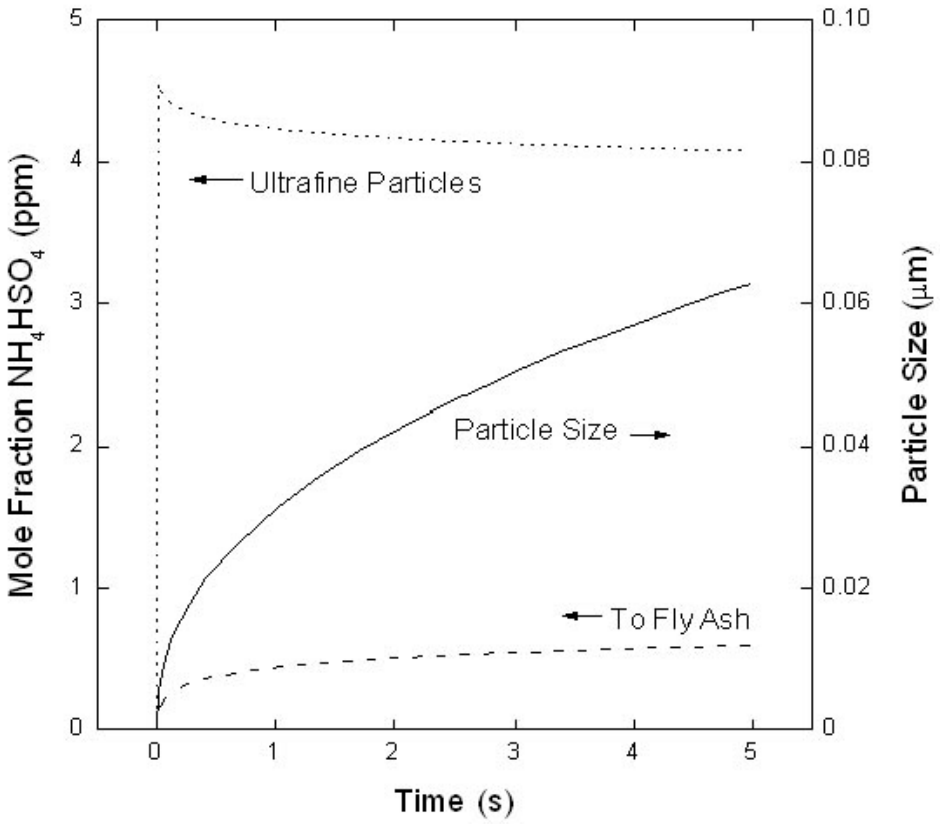

Figure 9. Evolution of the distribution of ammonium bisulfate between ultrafine particles and fly ash and growth of the ultrafine particles by coagulation during 5 s at 150 °C (302 °F), the time required for passage from the air preheater to the particulate control device. The processes occurring in the air preheater, shown in Figure 8b and Figure 8c, are compressed into the first 0.014 s at the left in this figure.

So the estimated contribution of ammonium bisulfate to the particle loading approaching the pollution control device (ESP) is 4 ppmv. This material would be distributed over a size range typically characterized by a geometric standard deviation of 1.32 for a self preserving size distribution in the free molecule regime.[37] Dismukes[4] found that, with injection of approximately 20 ppm ammonia, the number of particles measured with a condensation nuclei counter increased by factors of 3 to 4. Simultaneous measurements of ESP electrical parameters (voltages and currents) presented clear evidence of the effects of space charge, specifically a reduction of current for a given applied voltage. At three of four sites, ESP collection efficiency was improved. It was concluded that enhanced operation was associated with space charge combined with enhanced cohesion of fly ash in the collection

layer on ESP collection plates. Higher cohesion reduced fly ash reentrainment during rapping of the plates. Fly ash resistivity was not affected by ammonia injection although it has been postulated that ammonia injection caused increased resistivity in some instances.

The mechanism by which space charge enhanced ESP collection efficiency was not explained in the reports on the three sites mentioned above. In fact, the improvement is counter-intuitive as a reduction of ESP current would be expected to lead to reduced ESP performance. A mathematical model for ESP operation was used to evaluate the importance of this new aerosol mass (associated with SCR) on ESP performance to determine what change in performance should be expected from theory. The aerosol mode resulting from the above analysis was added to the inlet size distribution data of Figure 2. Then theoretical voltage-current (V-I) ESP operating points[2,3] were calculated using both the original inlet size distribution and the ammonium bisulfate augmented distribution. Model projections of ESP collection efficiencies were then calculated using the two corresponding size distributions and operating currents and voltages. The results, given in Figure 10, suggest there to be no concern at these ammonium bisulfate loadings. The results showed a substantial increase in space charge that reduced current at the projected operating voltage

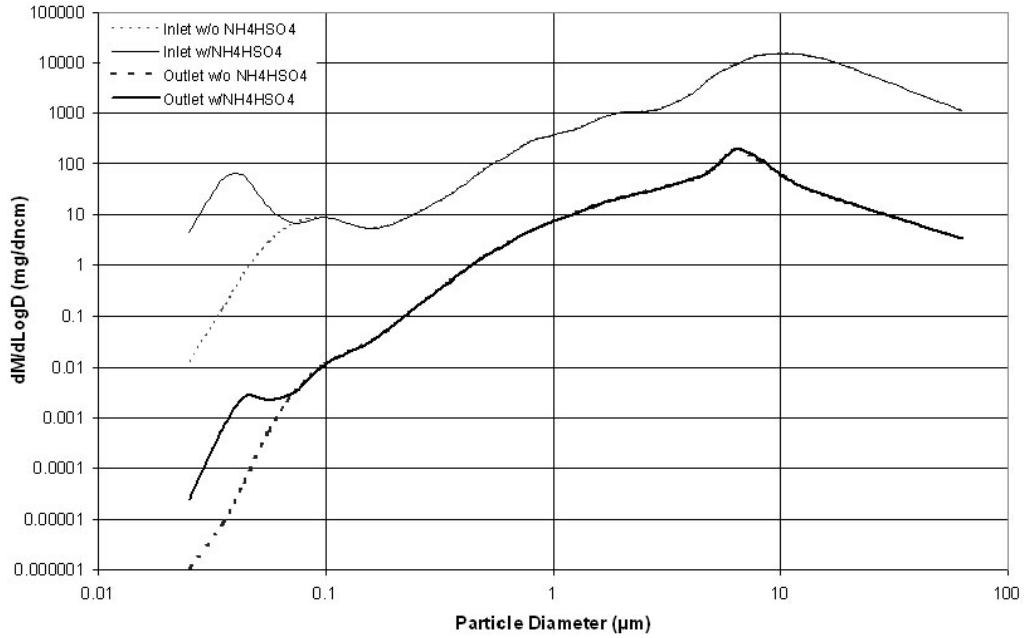

Figure 10. ESP inlet and outlet particle size distributions of fly ash with and without a nucleated ammonium bisulfate mode expected from downstream of an air preheater when an SCR is present. (The ESP inlet curve without ammonium bisulfate is measured data, and outlet distributions were calculated using an ESP model for a typical ESP.)

in the absence of the ammonium bisulate. However, increasing the applied voltage of the first ESP field from 36 to 43 kV brought current back to the level present without the ammonium bisulfate mode and somewhat improved collection such that predicted in-stack opacity decreased from 11 to 9%. The predicted outlet loading contained 0.76 mg/dncm more mass in the ultrafine mode, or 4.6×10^9 particles per cubic meter more with the ammonium bisulfate compared to the system without ammonium bisulfate. The calculated particle number loadings in this mode with ammonium bisulfate present are a factor of 38 higher than without ammonium bisulfate, but these particles would coagulate with the normal fly ash present so that any concern with this potential effect can be characterized as increased mass in this ultrafine mode.

The ability to increase applied voltage in the ESP analysis above is predicated on two issues. The first is associated with the resistivity of the fly ash layer. If the resistivity is high, the applied voltage is limited by sparking that originates from break down in the ash layer at some voltage differential across the layer. In the instances relevant here, resistivity will typically be lowered by installation of an SCR because of the increased net levels of SO_3. Otherwise, there is no mechanism known by which the resistivity would be increased. Therefore, the original (before SCR) or higher currents can exist for the same break down voltage differential across the layer. The second issue is the capability of the ESP power supply to produce higher applied voltages. Replacement with modern equipment may be necessary at a few installations.

The levels of ammonia slip considered here, for which no degradation of ESP performance is indicated, are expected to be representative of most SCR installations. If ammonia and SO_3 levels present at the air preheater inlet are allowed to be substantially larger, other problems may be encountered. Previous field tests have included such conditions in which ammonia was injected upstream of an ESP. Buildup of deposits of ammonium bisulfate particles on collection plates and corona electrodes that were not removed by normal rapping interfered with ESP performance. Similar consideration applies to baghouse operation. Previous experience when both ammonia and SO_3 concentrations were greater than 10 ppmv and when SO_3 concentration alone was greater than 10 ppmv indicated problems with degradation of fabric strength. Again, significant degradation associated with ammonia bisulfate is not expected at ammonia levels considered above (a few ppmv). However, levels of SO_3 greater than 10 ppmv, independent of ammonia, may be difficult to avoid with many SCR installations; although, as mentioned before, injection of hydrated lime at the baghouse inlet can be effective at preserving fabric strength.

5. Sulfuric Acid Aerosol Formation and Collection in Wet FGD

The gas-to-particle conversion processes that dominate transformation of sulfuric acid vapor to particulate matter in wet scrubbers are different than the analogous dominant processes typical for stack emissions in the absence of a wet scrubber. The rapid quench of the flue gas by water spray favors nucleation relative to the dilution cooling of acid vapor occurring as the result of mixing stack gas with ambient air. The particle size of nucleated acid in an FGD scrubber is governed by coagulation and absorption by acid of water vapor at essentially 100% relative humidity. The evolution of this nucleated aerosol can be illustrated directly by utilizing the self-preserving form of the size distribution associated with coagulation.[35] The decline of particle number concentration and the growth of average particle size are illustrated in Figure 11 for relative H_2SO_4/water concentrations of 50:50 by mass. These are the relative concentrations for equilibrium at scrubber temperature and 50% relative humidity. The time scale considered was derived from the assumption that residence time in a scrubber is a few seconds and in the associated stack may be tens of seconds, such as corresponding to an 800 ft stack. These results simulate an initial nucleation event followed by coagulation only. Subsequent growth by diffusion of water vapor to, and absorption by, acid droplets that actually occurs is not taken into account. As such, these calculations represent lower limits of droplet diameter in the stack. The actual growth in the stack from the saturated water vapor also enhances coagulation somewhat, leading to still larger droplet sizes than calculated. After leaving the stack and mixing with ambient air, the acid droplets dry and become considerably smaller. The 50:50 relative H_2SO_4/water concentration on which Figure 11 is based corresponds to 20 °C temperature and 30% relative humidity. At higher humidities, actual droplets retain more water relative to H_2SO_4 than the condition assumed for Figure 11. Figure 12 gives corresponding scattering coefficients and average specific scattering coefficients for the coagulating aerosols depicted in Figure 11. The calculated increase with time of particle size resulting from coagulation causes average specific scattering coefficients (γ^*_{ave}) to similarly increase with time and H_2SO_4 concentration. Figure 13 presents data of Figure 12 in terms of γ^*_{ave} versus H_2SO_4 concentration for fixed coagulation times as appropriate for a given site—specifically, residence time in the scrubber and stack. Average specific scattering coefficient is seen to increase with H_2SO_4 concentration , nearly following quadratic functions ($R^2 = 0.9987$). This means that the amount of light scattered by H_2SO_4 in scrubber plumes is calculated to increase with emission level faster than a simple linear dependence. This dependence is stronger for longer coagulation times.

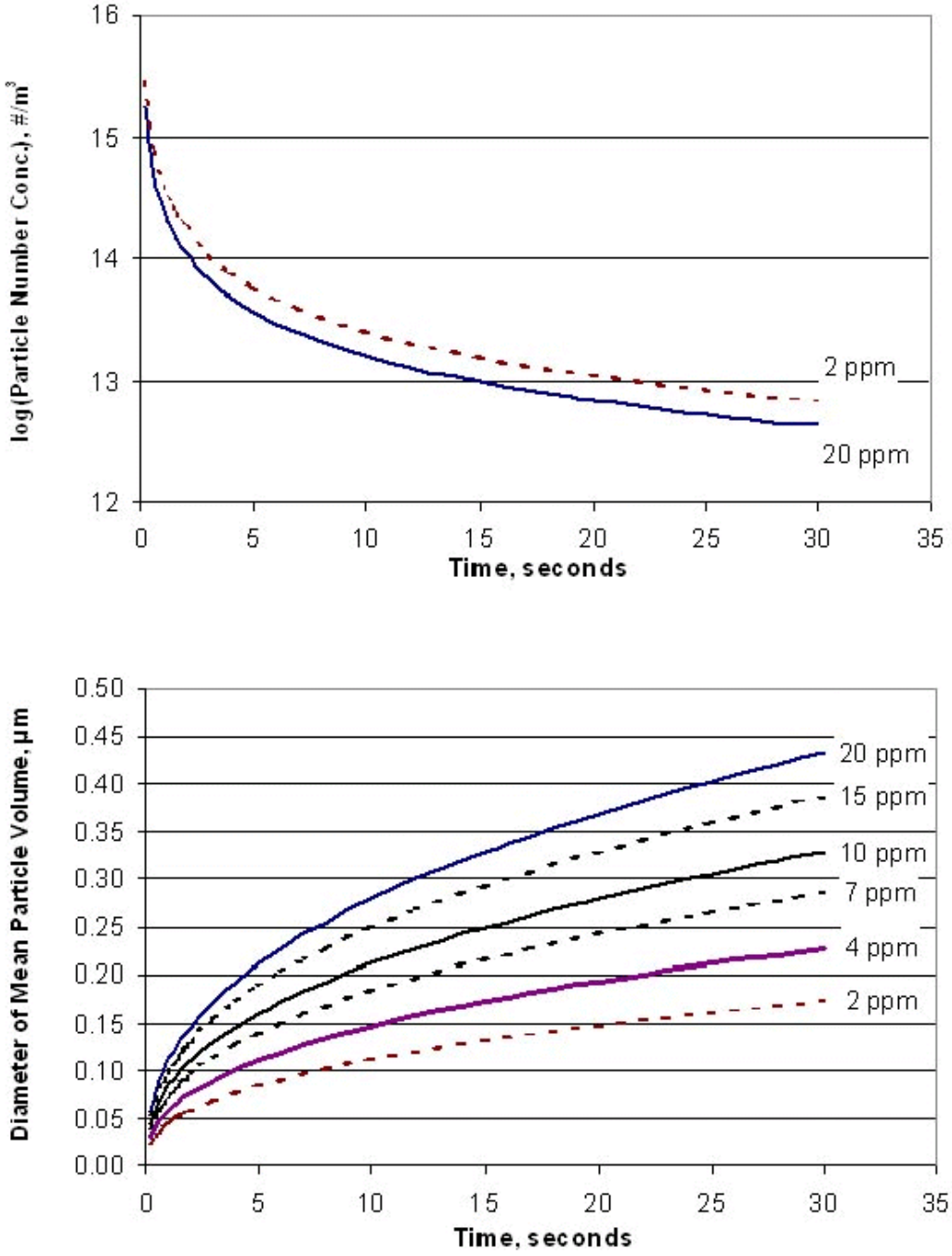

Figure 11. Growth by coagulation of nucleated sulfuric acid droplets from H_2SO_4 molecules. (This simulation is for a gas temperature of 20 °C, for which acid droplets are 35% H_2SO_4 and 65% H_2O by mass.)

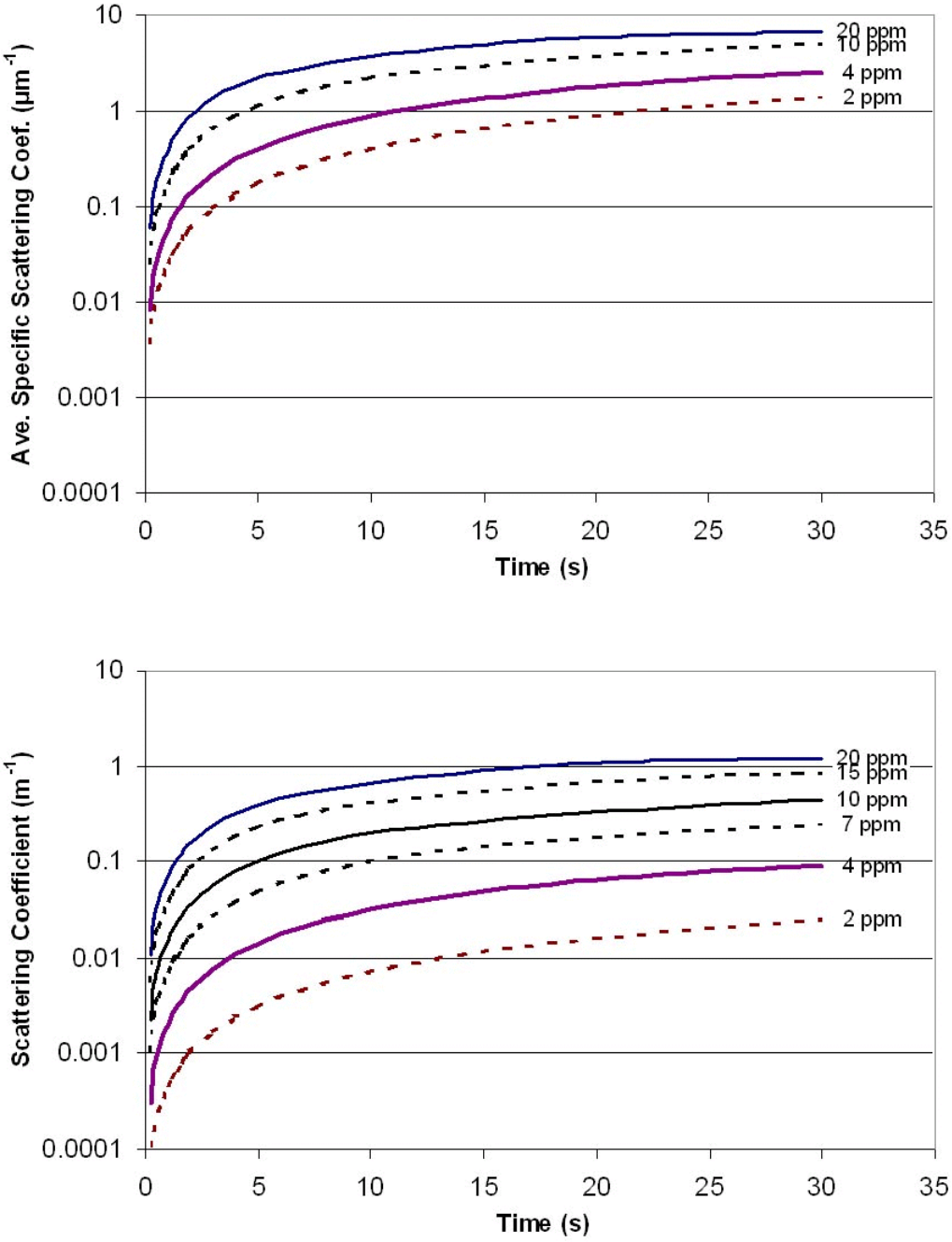

Figure 12. Scattering coefficients and average specific scattering coefficients of nucleated sulfuric acid droplets versus time for the various H_2SO_4 concentrations of Figure 11.

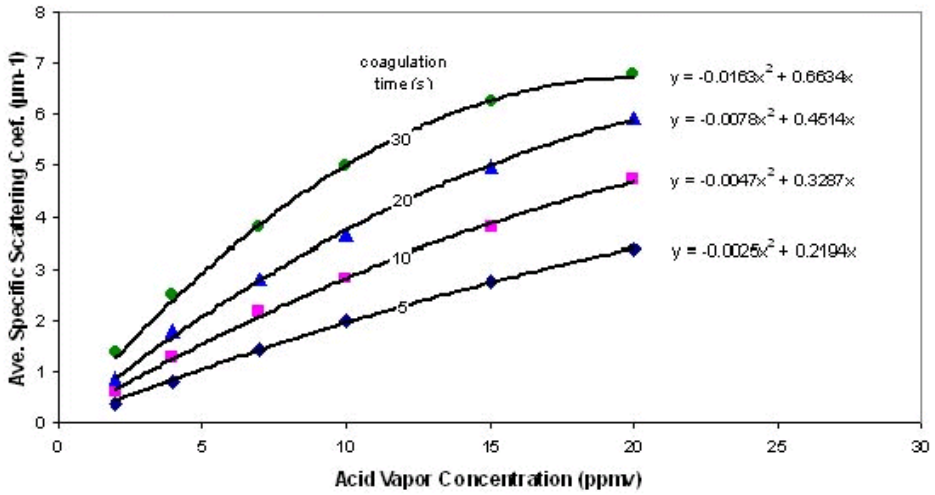

Figure 13. Average specific scattering coefficients of nucleated sulfuric acid droplets versus H_2SO_4 concentrations for various times from Figure 12.

Wet scrubbers utilized for SO_2 control incorporate little energy (equivalent to about 2 inches of H_2O pressure drop) into the relative motion of droplets and particles compared to that which leads to substantial collection of particles in high energy scrubbers. Energy input equivalent to at least 20 in. H_2O is necessary to achieve a 50% collection efficiency of 1µm particles.[49] Energy input of 2 in. H_2O can achieve 50% collection of particles about 4 µm diameter.[49] Data characterizing particulate collection efficiency of low energy scrubbers at particle sizes below 1 µm are not available. However, measurements on high energy scrubbers for sizes well below the 50% cut point show significant collection by turbulent and Brownian diffusion, leveling off at about 30%.[49] A recent investigation found acid removal efficiency (i.e., acid aerosol removal) at one site to be 77% with relative standard deviation of 0.09 initially. Six months later, repeat measurements resulted in 31% removal with relative standard deviation of 0.13 with no apparent reason for the variation.[50] In view of the previously measured data characterizing particle collection efficiency versus size and scrubber input energy, the 31% value appears plausible while the higher value does not. The higher value is believed to be associated with measurement problems of acid aerosols in scrubber effluent.

The overall behavior of plumes also differs substantially between that exiting a wet scrubber at temperatures well below 200 °F and that exiting a stack without a scrubber at temperatures on the order of 300 °F. Figure 14 presents results of plume modeling for

conditions typical of wet scrubber exhaust and summer days. Ground level concentrations of sulfuric acid are given versus downwind distance assuming 50 ppmv initial stack concentration of H_2SO_4. Mixing class A produces the most rapid vertical mixing and occurs only about one afternoon hour on several days of a typical summer month. Mixing classes B and C are more common, occurring for late morning/early afternoon hours on most summer days. Analogous modeling of plumes originating from flue gas in the stack at 300 °F predicts ground concentrations of zero over the same downwind distances because the buoyancy of the hot gas causes the plume to penetrate through the top of the mixing layer, preventing contact of the plume with the ground.

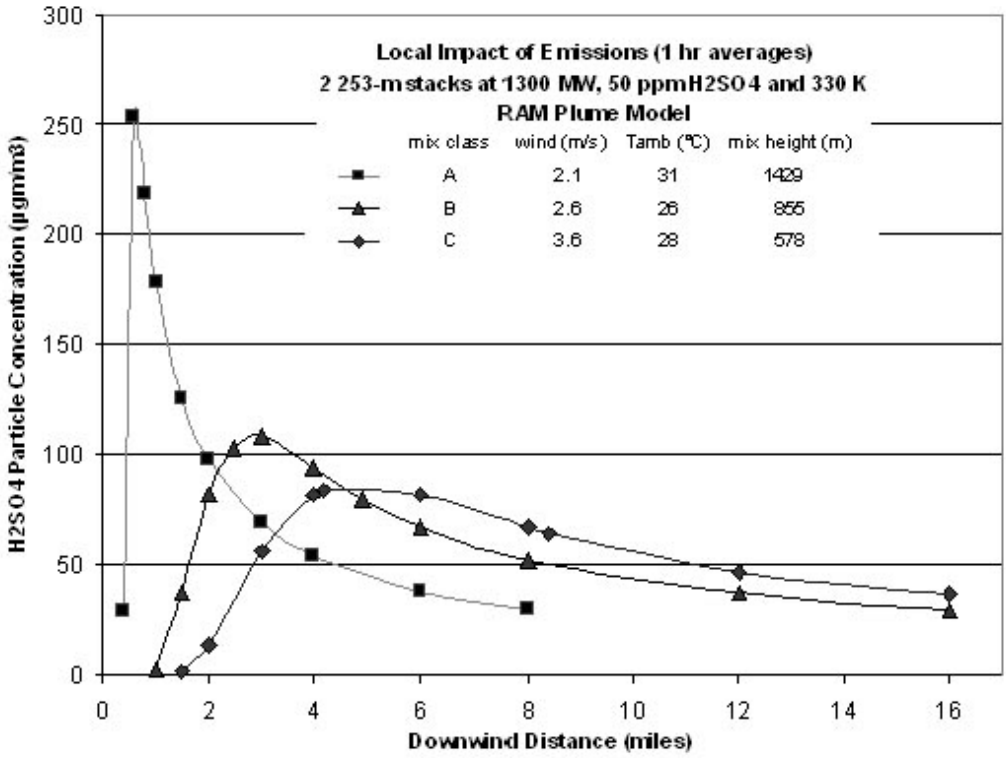

Figure 14. Predicted ground level concentrations of particulate H_2SO_4 for illustrative conditions representing a stack effluent exhausting a wet scrubber for SO_2 control of coal-fired boiler emissions.

6. SO_3/H_2SO_4 Measurement and Monitoring

Method 8, the EPA promulgated method for measuring emissions of sulfuric acid mist,[51] has a detection limit of about 50 mg/m^3; thus, it lacks the sensitivity needed for measurements at electric utility plants. The controlled condensation method (CCM) developed by Cheney and Homolya[52] is generally recognized as the most reliable method for measuring SO_3/H_2SO_4 at the levels encountered at power plants.[52,53] In the CCM, a sample gas stream is conveyed through a heated quartz-lined probe, through a quartz fiber filter, and then through a condenser in which the acid vapor is removed from the sample gas stream. The probe and filter holder are held at a temperature at or above 288 °C (550 °F), hot enough to evaporate concentrated H_2SO_4 that may be in the liquid or adsorbed phase. The condenser is maintained at a temperature above the moisture dew point but well below the sulfuric acid dew point so that all of the acid is collected in it. A second filter downstream of the condenser ensures that any acid aerosolized in the condenser is retained for analysis with that collected in the condenser itself.

Over the past few years, potential improvements in the CCM method as it is applied to coal-fired utility installations have been investigated.[6,50] One of the major difficulties in SO_3/H_2SO_4 sampling is separation of fly ash and other extraneous particulate matter. In principle, this is accomplished with the heated quartz fiber filter with condensed phase H_2SO_4 being evaporated and transferred to the condenser. However, both condensed and vapor phase H_2SO_4 can react with collected particles due to the resulting intimate contact while passing through the filter and any deposits on it, resulting in a negative bias in the measurement. This artifact was evaluated in laboratory studies by passing known levels of H_2SO_4 vapor through filters prepared with representative fly ash deposits.[6] The importance of the reaction was found to vary with alkali content. That is, fly ash from coals normally associated with high SO_3 levels did not produce a significant bias.

The primary improvement implemented in recent investigations of the method has been use of 10-ft probes to assure that condensed or adsorbed H_2SO_4 in the sample gas is entirely volatilized in the probe before reaching the filter upstream of the condenser.[50] The latter problem is especially relevant when downstream of a scrubber where the H_2SO_4 is entirely in the condensed phase. This sampling train was utilized in the field results discussed above concerning removal efficiency of H_2SO_4 by wet FGD. As discussed above, there remains concern with the sampling method due to the large variation of field measurement of H_2SO_4 removal (30% to 80%) and the inability to explain high removal efficiency by mechanisms involved in wet FGD scrubbers.

It is generally assumed that H_2SO_4 not in the vapor state is essentially all comprised of particles that are small enough that isokinetic sampling is not required in order to obtain a representative sample. Further, it is generally assumed that complete spatial traverses of the ducts (or stacks) are not required, although traversing of representative temperature zones, especially immediately downstream of air preheaters, is required. Data obtained in field measurement programs conducted by SRI over the past few years calls into question the assumptions regarding the lack of need for isokinetic sampling and traversing. As part of programs for diagnosing plume opacity problems at several coal-fired power plants, SRI has developed a technique for determining the size distributions of the stack particulate emissions in terms of the contributions of coal fly ash, scrubber generated solids, sulfuric acid, and combined water.[54] The technique uses a sophisticated set of chemical and gravimetric analyses of in situ, size-fractionated samples obtained using cascade impactors fitted with inertial precollectors. Although the technique is still experimental and remains under development, some results obtained with it suggest that the assumption may not be valid that the sulfuric acid in the stack is entirely in the form of particles small enough that isokinetic sampling is not necessary. Figure 15 illustrates the data obtained during one such test.[54] In this case, about 80% of the acid appears to have been associated with particles larger than 10 μm. Data obtained during a second test at the same location showed comparable concentrations of sulfuric acid at sizes below about 10 μm, but the peak between 10 and 100 μm was comparable in size to that near 0.1 μm in Figure 15, meaning it showed 50% of the acid was associated with relatively large particles. The CCM as it is conventionally applied would tend to grossly under-sample particles larger than 1 μm and might not be capable of volatilizing those that were sampled. Thus, the data shown here suggest that sulfuric acid concentration results at scrubber outlets obtained to date may have been biased low by significant amounts. Further, the variability in the concentrations at sizes greater than 10 μm may explain part of the large variability in sulfuric acid collection efficiencies measured across scrubbers.

If the CCM is to be used at such locations, a traversing capability may be needed together with the addition of a precollector such as that used with cascade impactors. The use of isokinetic sampling in conjunction with the added precollector may significantly improve the results. The precollector catch can be analyzed for acid in the same fashion as that used in obtaining the data shown in Figure 15, closing the gap in the data without incurring the large expense incurred in analyzing the many size fractions obtained with cascade impactors.

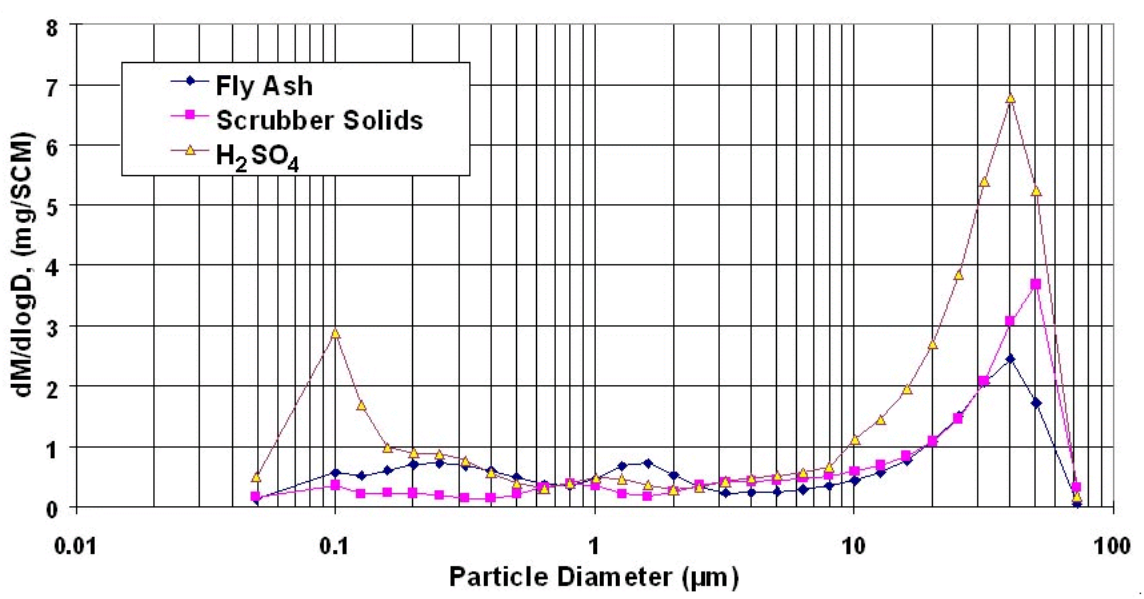

Figure 15. Concentration vs particle size for fly ash constituents, scrubber solids constituents, and sulfuric acid measured in the stack of a coal-fired utility boiler whose emissions were controlled by an ESP followed by a wet scrubber.[54]

An accurate and reliable sulfuric acid monitor would greatly facilitate control of SO_3 at coal-fired boilers. Several monitors have been developed over the years, some using colorimetric methods (e.g., the Severn Science Ltd. System), spectroscopic techniques (e.g., the tunable diode laser system first developed by Laser Analytics), and a conductivity cell system developed by the U.S. EPA.[55] Physical Sciences Incorporated has announced the intention to develop an IR spectroscopic-based analyzer.[56] Ametek Process Instruments is developing a prototype SO_3 monitor based on their commercial Model 4600 SO_2 Analyzer.[57] Ametek states that their prototype monitor uses a chemical reaction with the SO_3 in a sample gas stream, "permitting a simple turbidity measurement proportional to the SO_3 concentration." Instrumental H_2SO_4 measurement in coal-fired boilers has been limited while the CCM continues to be more widely used. It is believed that, as with the CCM, difficulties associated with separation of H_2SO_4 from fly ash and other entrained particulate matter must be solved.

The Severn Science system has shown promise in laboratory evaluations[58,59] and has been available commercially for many years. In two field evaluations of the Severn Science unit on boilers burning residual fuel oil when sampling at the air preheater inlets, measurement error was typically found to be less than 10% compared to controlled condensation methods.

However, evaluation on a coal-fired boiler led to inconsistent results with fluctuations that could not be explained.

7. CONTROL TECHNOLOGY ISSUES

The degree of additional control for fine PM which may be required as a result of SCR installation will vary greatly depending upon the fuel, boiler design, SCR system design, and the pollution control system configuration. Table 3 represents an attempt to categorize the major types of installations that are expected to be encountered in the utility PC boiler population. Control technology requirements and options are listed beside each major system category.

Table 3. System Categorizations

Description of System with SCR	Fine PM Control Technology Options
Low S Western coal with fabric filter or SD plus fabric filter	None required
Low S Western coal with ESP	Probably none required with high alkaline ash—otherwise reduce temperature ahead of ESP so H_2SO_4 condenses to be caught in ESP
Low to medium sulfur Eastern coal with ESP or fabric filter	Probably none if PCD operates <250 °F— otherwise reduce temperature ahead of ESP so H_2SO_4 condenses to be caught in PCD, sorbent injection. May require upgrade of ESP if it is an older unit with an SCA of ~300 or less.
Eastern coal with hot-side ESP plus wet scrubber	Furnace sorbent injection, sorbent downstream from SCR, or wet ESP after scrubber
Eastern coal with cold-side ESP plus scrubber	Sorbent injection, otherwise reduce temperature ahead of ESP so H_2SO_4 condenses to be caught in ESP. May require upgrade of ESP if it is an older unit with an SCA of ~300 or less. Alternatively, install wet ESP after scrubber
Any coal with spray dryer and cold-side ESP	Probably none but may require upgrade of ESP if it is an older unit with an SCA of ~300 or less.

As indicated previously in this report, ammonium compounds resulting from SCR use are likely to form at temperatures above normal ESP operating temperatures. Therefore, if the ESP is operating with the high collection efficiency (greater than 99.5%) required for most particulate emission regulations, the ammonia compounds should be collected in the ESP with greater than 75% efficiency, as suggested by the analysis in Section 3, and are not likely to cause plume visibility problems. The ammonia slip, as previously noted, is normally limited to 2 ppmv to avoid problems with fly ash sale or disposal.

The most difficult fine PM emission problems will occur when H_2SO_4 vapor or aerosol concentrations leaving the ESP or the wet scrubber exceed the equivalent of 2 ppmv. These

concentrations have the potential to form aerosols in the plume that will have an adverse effect on plume visibility and appearance. Extensive work has been performed on injection of alkaline sorbents—especially magnesium compounds—to react with SO_3 or H_2SO_4 vapor upstream of the ESP so that the vapor is converted to PM which is collected in the ESP.[60] Although many of these trials have been successful in removing the sulfuric acid vapor, long term side effects of the injection process are still an area of concern. The effect of the sorbent on the catalyst—if injected upstream of the SCR or in the furnace—is one potential problem area. Another potential difficulty is adverse effects on ESP performance if the electrical resistivity of the ash is raised above the desired value for optimum electrical operation.[47]

Wet ESPs downstream from the wet scrubber are receiving increased attention.[61] Wet ESPs are capable of collecting the fine PM that may result from SCR generated sulfuric acid. However, uncertainties remain in defining the efficiency of collection that would be required to maintain appropriate emission levels and in identifying a wet ESP design configuration that can reliably maintain the fine PM concentration below visible threshold limits.

The potential plume visibility problem discussed herein is, of course, exclusively concerned with fine PM. Therefore, it is of interest to summarize a recent data review performed on PCD performance in collecting particles below 2.5 and 1.0 micrometers aerodynamic diameter.[62] Figure 16 contains a bar chart illustrating fine PM concentrations—at both 1.0 and 2.5 micrometers aerodynamic diameter—at system outlets for several systems treating flue gas from utility power boilers. Also shown are outlet fine PM concentrations from two pilot plant experimental programs (COHPAC II, ESFF).[63,64] This graph was prepared using cascade impactor data obtained by sampling with traverses at each control device outlet sampling location. The data on the full-scale systems were collected during various field measurement projects dating back as far as 1975.

Figure 16 displays cumulative mass concentrations at 1.0 and 2.5 micrometers aerodynamic diameter normalized to milligrams per dry normal cubic meter (mg/dnm^3 - 0% water, 20 °C) at 0% oxygen for the various systems (aerodynamic diameters are based on unit density aerosols). The first set of bars for the “E&S” system illustrate the quantity of fine PM measured by the impactor sampling systems when a sulfuric acid fume had formed in the scrubber system downstream from a high efficiency ESP.[39] Ammonia injection upstream of the precipitator has been used at this site to minimize the quantity of sulfuric acid vapor that is available to condense in the scrubber.

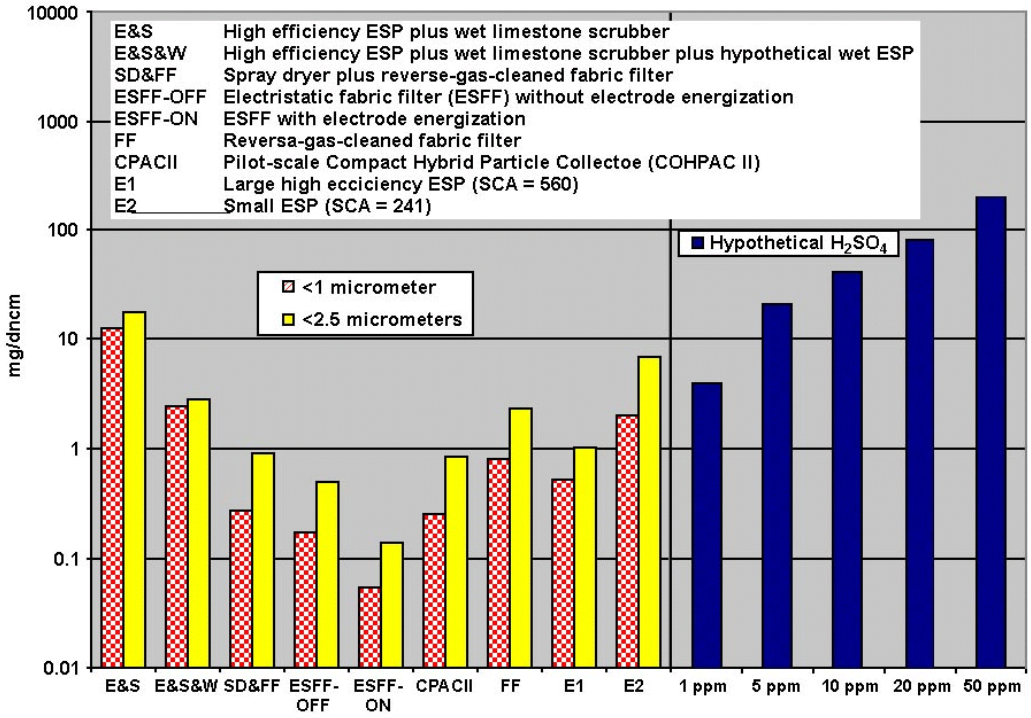

Figure 16. Fine PM concentrations on a cumulative mass basis for several pollution control systems. The equivalent mass concentrations for hypothetical SO_3 emissions at 1, 5, 10, 20, and 50 ppmv are shown for comparison and are not directly associated with any specific control system.

The second set of bars (E&S&W) are calculated results based on experiments on a pilot-scale wet ESP.[65] Wet ESPs are designed to operate in saturated gas streams. In this hypothetical configuration, a wet ESP is installed downstream of a wet scrubber, and the particulate collection efficiency as a function of particle size is assumed to be the same as that measured in the pilot scale experiments. The calculated results indicate the cumulative mass emissions below 2.5 micrometers are reduced by 83%. This result is based on a small wet ESP (specific collection area of approximately 35 ft^2/1000 acfm) intended for use as a polishing device behind a dry ESP that does not meet current emission requirements. It is reasonable to expect that a wet ESP optimized for operation downstream of a scrubber could achieve higher collection efficiencies than those used for this hypothetical example.

The spray-dryer plus fabric-filter combination in Figure 16 (SD&FF) achieved the lowest fine PM concentrations among the full-scale systems tested.[5] The full-scale fabric filter

without a spray-dryer upstream (FF) used bags which had been in service for several years, and the fine PM emissions measured at that location may have been increased by leaks through the bags or in the baghouse structure.[66] Both of these full-scale fabric filter installations, however, indicated cumulative mass efficiencies of greater than 99% for aerodynamic particle diameters smaller than 1 μm.

The full-scale precipitator (E1) was a large SCA unit (560 ft^2/1000 acfm) collecting ash from a low-sulfur western coal that produced an ash with an electrical resistivity that did not cause problems with electrical operation. Overall particulate mass emissions at this plant were very low—approximately 2.48 mg/dnm^3 at 0% O_2 (0.0015 lb/million Btu).[67]

The second full-scale ESP illustrated in Figure 16 (E2) is perhaps more typical of older units with smaller specific collection areas, in this case 241 ft^2/1000 acfm.[67] Note that the PM 1.0 and 2.5 concentration values are much higher than for E1 and higher than any of the fabric filters in this comparison.

The full-scale fabric filter (FF) data are based on tests conducted at a large plant burning a western subbituminous coal. It is typical of the large, low-ratio, reverse-gas-cleaned baghouses found on many plants in the western United States. Its fine particle collection performance is adequate, falling between the two electrostatic precipitator examples shown (E1 and E2).

Figure 16 also illustrates outlet fine PM concentrations from two pilot-scale fabric filter systems:

1. An experimental electrostatic fabric filter (ESFF) without power (ESFF-OFF) and with power applied to the discharge electrodes (ESFF-ON),[62] and
2. A Compact Hybrid Particle Collector (COHPAC II) pilot (CPACII in Figure 16).[63]

The COHPAC II pilot unit consisted of a two-field ESP operated at about 188 ft^2/1000 acfm followed by a pulse-jet baghouse that was operated at an A/C ratio ranging from 10.4 to 11.2 ft/min. The average tube sheet pressure drop ranged from 4.6 to 6.6 inches of water.[63]

All of these pilot-scale fabric filter configurations achieved very low outlet fine PM concentrations-less than 1.0 mg/dnm^3 at 0% O_2. The ESFF power-on configuration achieved the lowest values, and the value of 0.05 mg/dnm^3 for cumulative mass below 1.0 μm was at the lower limit of resolution for cascade impactor sampling systems under the conditions of these tests.

Note that the bars labeled "Hypothetical H_2SO_4" represent the mass concentration equivalent of H_2SO_4 concentrations ranging from 1 to 50 ppmv. The graph illustrates that only 5 ppmv H_2SO_4 is equivalent to more mass in the sub-2.5 μm range than was measured at the outlet of any of the sources depicted, the greatest being the ESP-wet scrubber combination. It was apparent that condensation was occurring across the scrubber during the measurement program because negative collection efficiencies were observed below 1 μm aerodynamic diameter.

We can derive some practical implications concerning plume appearance from the data in Figure 16. Let us assume that SCR introduced an increase of 10 ppmv sulfuric acid vapor which was reduced to 6 ppmv in passing through the air preheater and down to 4.5 ppmv through the ESP. This 4.5 ppmv acid is expected to nucleate in the scrubber. As discussed in Section 4, we expect penetration of 70% of this aerosol (3 ppmv) to the stack based on the low pressure drop of wet FGD scrubbers. Due to the saturated water conditions in the scrubber, the nucleated acid droplets will grow and coagulate until they exit the stack where drying proceeds slowly to a stable point at which acid content of the droplets is about 50% by weight,[35] or 1/3 acid and 2/3 water by volume. The optical depth (γL) of the plume declines slowly, so a reasonable estimate of the scattering coefficient is derived from using a dilution factor of L/L(z) where z is the distance traveled and L(z) is the cross wind depth of the plume. If the stable particle size were 0.1, 0.2, or 0.3 μm, the scattering coefficient would be 0.006, 0.04, or 0.08 L/z m^{-1}, respectively. The value for 0.1 μm average particle size appears realistic. If the stack diameter were 10 m, the plume opacity would be 6%, a readily visible haze but not unusual. The average particle size is unlikely to be less than 0.1 μm. These estimates of scattering coefficient and opacity should be considered to be linear with respect to sulfuric acid concentration in the stack—that is, doubling the SO_3 concentration would double the opacity.

Additional control above that provided by current practice will likely be needed in many instances to handle increased levels from SCR. Further, subtleties related to particle growth that cannot be accounted for at present might cause formation on, or condensation to, larger particle sizes (0.2 or 0.3 μm) that would result in larger scattering coefficients than those predicted here. A control level of 80% is not an unreasonable expectation for total fine PM. Pilot scale wet ESP measurements have indicated more than 80% cumulative mass collection efficiency for particles below 0.5 μm aerodynamic diameter.[5] It is possible that a combination of modest amounts of sorbent injection combined with a small-footprint wet ESP could provide a margin of safety for adverse plume appearance events that may result from SCR-induced sulfuric acid concentration spikes or fuel changes at plant sites with

ESP-scrubber control systems.

In conclusion, this review indicates control technologies are available that have the potential to largely eliminate adverse plume appearance resulting from application of the SCR process. The difficulty faced by utility plant operators is that guidelines are not presently available to define the extent of the problem that may occur at a given site. In the absence of such guidelines, it is not possible to determine in advance the control strategies that are technically and economically feasible for a particular plant site.

8. References

1. Downing, B. “Power Plant Releases Clouds Of Sulfuric Acid,” *Akron Beacon Journal*, p. A1: Akron, OH, August 2, 2001.
2. Faulkner, M.G., and DuBard, J.L. “A Mathematical Model of Electrostatic Precipitation (Revision 3): Volume I. Modeling and Programming,” U.S. EPA Industrial Environmental Engineering Laboratory, EPA-600/7-84-069a [NTIS PB84-212679]: Research Triangle Park, NC, June 1984.
3. Faulkner, M.G., and DuBard, J.L. “A Mathematical Model of Electrostatic Precipitation (Revision 3): Volume II. User’s Manual,” U.S. EPA Industrial Environmental Engineering Laboratory, EPA-600/7-84-069b [NTIS PB84-212687]: Research Triangle Park, NC, June 1984.
4. Dismukes, E.B. “Conditioning of Fly Ash with Ammonia,” *J. Air Poll. Control Assoc*. 25(2): 152-156, 1975.
5. Gooch, J.P., and Sedman, C.B. “Advanced Particulate Control and Implications Toward Solving Multiple Pollutant Control Problems in Coal-Fired Boilers,” Proceedings of the EPRI-DOE-EPA Combined Utility Air Pollutant Symposium: Washington, D.C., August 1997.
6. Blythe, G., Galloway, C., Richardson, C., and Rhudy, R. “Improvements to the Controlled Condensation Measurement Method for Sulfuric Acid,” Proceedings of the EPRI-DOE-EPA Combined Utility Air Pollution Control Symposium: Atlanta, GA, 1999.
7. Malm, W.C. “Introduction to Visibility,” National Park Service, T097-04, T098-06, 1999.
8. Hardman, R., Stacy, R., and Dismukes, E. “Estimating Sulfuric Acid Aerosol Emissions From Coal-Fired Power Plants,” Proceedings of the U. S. Dept. of Energy (FETC) Conference on Formation, Distribution, Impact, and Fate of Sulfur Trioxide in Utility Flue Gas Streams: March 1998.
9. Walsh, P.M. “Properties of Particles Formed During Combustion of Residual Fuel Oils,” Research Report. EP90-15, Empire State Electric Energy Research Corp.: New York, NY, 1996.
10. Graham, K.A. and Sarofim, A.F. “Inorganic Aerosols and Their Role in Catalyzing Sulfuric Acid Production in Furnaces,” *J. Air & Waste Manage. Assoc*. 48: 106-112, 1998.
11. Walsh, P.M., Mormile, D.J., and Piper, B.F. “Sulfur Trioxide Formation in the Presence of Residual Oil Ash Deposits in an Electric Utility Boiler,” American Chemical Society, Division of Fuel Chemistry, Preprints, Vol. 38, No. 1, pp. 294-300.

12. Walsh, P.M., DeJohn, T.E., Bower, E.T., and Rahimi, M. “Measurements of Sulfur Trioxide and Sulfate in the Products of Coal Combustion in a Traveling-Grate Stoker,” NYSEG Report, Fuel Science Program, Penn. State University: University Park, PA, 1994.
13. Neville, M. “Current Research at the Energy Laboratory,” Massachusetts Institute of Technology, pp. 1-2: Cambridge, MA, 1983.
14. Cushing, K. M., Heaphy, R.A., and Dismukes, E.B. “Effects of SCR Ammonia on Ammonia Volatilization, Ammonia Extraction, and Metals Extraction from SCR Fly Ash,” Southern Research Institute Report Number SRI-ENV-95-415-7613: Birmingham, AL, October 1995.
15. Monroe, L.S., and Harrison, K.E. “An Updated Method for Estimating Total Sulfuric Acid Emissions from Stationary Power Plants,” Southern Company Services (Research and Environmental Affairs Department): Birmingham, AL, March 2003.
16. Quann, R.J., and Sarofim, A.F. “Vaporization of Refractory Oxides During Pulverized Coal Combustion,” Proceedings of the Nineteenth Symposium (International) on Combustion, The Combustion Institute, pp. 1429-1440: Pittsburgh, PA, 1982.
17. Senior, C.L., and Flagan, R.C. “Synthetic Chars for the Study of Ash Vaporization,” Proceedings of the Twentieth Symposium (International) on Combustion, The Combustion Institute, pp. 921-929: Pittsburgh, PA, 1984.
18. Helble, J., Neville, M., and Sarofim, A.F. “Aggregate Formation from Vaporized Ash During Pulverized Coal Combustion,” Twenty-First Symposium (International) on Combustion, The Combustion Institute, pp. 411-417: Pittsburgh, PA, 1986.
19. Sarunac, H., and Levy, E. “Factors Affecting Sulfuric Acid Emissions From Boilers,” Proceedings of the EPRI-DOE-EPA Combined Utility Air Pollution Control Symposium, Volume 1, Session 5, pp 1-11: Atlanta, GA, August 1999.
20. DeVito, M.S., and Oda, R.L. “Flue Gas Stratification at ESP Inlets,” Proceedings of the U. S. Dept. of Energy (FETC) Conference on Formation, Distribution, Impact, and Fate of Sulfur Trioxide in Utility Flue Gas Streams, March 1998.
21. Oglesby, Jr., S., and Nichols, G.B. *Electrostatic Precipitation*, Marcel Dekker, Inc.: New York, NY, 1978.
22. Zhang, Z. “Mass Transfer Processes In Flow Passages Of Rotating Regenerative Air Preheaters,” Lehigh University: Bethlehem, PA, Dissertation, 1991.
23. Verhoff, F., and Banchero, J. “Predicting Dew Points of Flue Gases,” *Chemical Engineering Progress*, 70: 71-79, 1974.
24. McCain, J.D., and Altman, R.F. “Improvements in Predicting the Effects of Sulfur Trioxide Vapor on Fly Ash Resistivity,” Proceedings of the 8th International Conference on Electrostatic Precipitation, Volume 2, Session C4, Paper C4-4:

Birmingham, AL., May 2001

25. Carr, R.C., and Smith, W.B. “Fabric Filter Technology for Utility Coal-Fired Power Plants, Part II: Application of Baghouse Technology in the Electric Utility Industry,” *J. Air Pollut. Control Assoc*. 34(2): 178-185, 1984. Also in Electric Power Research Institute Special Report EPRI CS-3724-SR: Palo Alto, CA, October 1984.
26. Carr, R.C., and Smith, W.B. “Fabric Filter Technology for Utility Coal-Fired Power Plants, Part III: Performance of Full-Scale Utility Baghouses,” *J. Air Pollut. Control Assoc*. 34(3): 281-293, 1984. Also in Electric Power Research Institute Special Report EPRI CS-3724-SR: Palo Alto, CA, October 1984.
27. Carr, R.C., and Smith, W.B. “Fabric Filter Technology for Utility Coal-Fired Power Plants, Part V: Development and Evaluation of Bag Cleaning Methods in Utility Baghouses,” *J. Air Pollut. Control Assoc*. 34(5): 584-599, 1984. Also in Electric Power Research Institute Special Report EPRI CS-3724-SR: Palo Alto, CA, October 1984.
28. Merritt, R.L., and Bush, P.V. “Demonstration of Strategies for Improved Baghouse Performance at the Brunner Island Steam Electric Plant,” Final Report for EPRI and Pennsylvania Power & Light Company, Southern Research Institute, SRI-ENV-92-349-7072, April 1992.
29. Carr, R.C., and Smith, W.B. “Fabric Filter Technology for Utility Coal-Fired Power Plants, Part IV: Pilot-Scale and Laboratory Studies of Fabric Filter Technology for Utility Applications,” *J. Air Pollut. Control Assoc*. 34(4): 399-413, 1984. Also in Electric Power Research Institute Special Report EPRI CS-3724-SR: Palo Alto, CA, October 1984.
30. ASTM International, ASTM Method D3786-01. “Standard Test Method for Hydraulic Bursting Strength of Textile Fabrics,” Book of Standards, Vol. 07.02 (D13.59).
31. Heaphy, R.F., and Cushing, K.M. “Evaluation of the 10-MW High-Sulfur Fabric Filter Pilot Facility, Volume II: Shake Deflate Cleaning and Fabric Testing,” Southern Research Institute, Final Report, Proj. 5000. EPRI CS-6061, Vol. 2, December 1991.
32. Felix, L.G., Merritt, R.L., and Duncan, K.S. “Improving Baghouse Performance at the Monticello Generating Station,” *J. Air Pollut. Control Assoc*. 36(9): 1075-1085, 1986.
33. Bush, P.V., Duncan, K.S., and Chang, R.L. “Improving Baghouse Performance at the Monticello Steam Electric Station with Ammonia and SO_3 Conditioning,” Proceedings, Ninth Particulate Control Symposium, Volume 2: Baghouses and Advanced Particulate Control Technologies, Session 4B, Paper 13-1, EPRI TR-100471, 2, Electric Power Research Institute: Palo Alto, CA, 1992.
34. Dismukes, E.B. “Trace Element Control in Electrostatic Precipitators and Fabric Filters,” *Fuel Processing Technology*, 39: 403-416, 1994.

35. Friedlander, S.K. *Smoke, Dust and Haze: Fundamentals of Aerosol Behavior*, p 204 Wiley: New York, 1977.
36. McCain, J.D., Gooch, J.P., and Smith, W.B. "Results of Field Measurements of Industrial Particulate Sources and Electrostatic Precipitator," *J. Air Pollut. Control Assoc*. 25(2): 117-121.
37. Lee, K.W., Chen, H., and Gieseke, J.A. "Log-Normally Preserving Size Distribution of Brownian Coagulation in the Free-Molecule Regime," *Aero. Sci. & Tech.* 3: 53-62, 1984.
38. Smith, W.B., Cushing, K.M,, Johnson, J.W., Parsons, C.T., Williamson, A.D., and Wilson, R.R. "Sampling and Data Handling Methods for Inhalable Particulate Sampling," EPA-600/7-82/036 [NTIS PB82-249897], U.S. Environmental Protection Agency Industrial Environmental Research Laboratory: Research Triangle Park, NC, May 1982.
39. Williamson, A.D., McCain, J.D., Smith, W.B., and Harris, D.B. "A Stack Dilution Sampling System for the Measurement of Condensable Vapors in Process Emissions," EPA-600/9-89-004 [NTIS PB89-166615], U.S. Environmental Protection Agency Air and Energy Engineering Research Laboratory: Research Triangle Park, NC, February 1989.
40. McCain, J.D., Kistler, W.F., and Carnes, D.H. "Impact of Primary Sulfate and Nitrate Emissions from Selected Major Sources. Phase 1. Coal-Fired Power Plant," EPA-600/3-85/066 [NTIS PB86-103678], U.S. Environmental Protection Agency Atmospheric Sciences Research Laboratory: Research Triangle Park, NC, September 1985.
41. DeFries, T.H. "Power Plant In-Stack and Near-Stack Plume Opacity: An Estimating Workbook," EPRI Report No. TR-104425, Electric Power Research Institute: Palo Alto, CA, October 1994.
42. Damle, A.S., Ensor, D.S., and Sparks, L.E. "Prediction of the Opacity of Detached Plumes Formed by Condensation of Vapors," *Atmos. Env*. 8(2): 435-444, 1984.
43. Damle, A.S., Ensor, D.S., and Sparks, L.E. "Options for Controlling Condensation Aerosols to Meet Opacity Standards" *J. Air Pollut. Control Assoc*, 37(8): 925-933, 1987.
44. Cichanowicz, J.E., and Muzio, L.J. "Twenty-Five Years of SCR Evolution: Implications For US Application And Operation," Proceedings of the AWMA 2001 Mega Symposium, Session 5, Paper 286: Chicago, Il, August 2001.
45. Hinton, W.S. "Demonstration of Selective Catalytic Reduction Technology for the Control of Nitrogen Oxide Emissions from High-Sulfur, Coal-Fired Boilers," DOE/PC/89652-T19 Vol. 1, U.S. Department of Energy: Morgantown, WV, 1996.

Also in “DOE Innovative Clean Coal Technologies Program,” Report SCS C-91-000026, Southern Company Services: Birmingham, AL.

46. Pritchard, S., DiFrancesco, C., Kaneko, S., Kobayashi, N., Suyama, K., and Lida, K. “Optimizing SCR Catalyst Design and Performance for Coal-Fired Boilers,” Proceedings, EPA/EPRI 1995 Joint Symposium of Stationary Combustion NO_X Control, May 1995.
47. Peterson, J.R., Jones, A F., Meserole, F.B., and Rhudy, R.G. “SO_3 Removal From Flue Gas by Sorbent Injection: EPRI HSTC Phase II Test Results,” Proceedings of the EPRI-DOE-EPA 1993 SO_2 Control Symposium, Session 6B, Paper 2: Boston, MA, August 1993.
48. Burke, J.M., and Johnson, K.L. “Ammonium Sulfate and Bisulfate Formation in Air Preheaters,” EPA-600/7-82-025a [NTIS PB82-237025], U.S. Environmental Protection Agency Industrial Environmental Research Laboratory: Research Triangle Park, NC, April 1982.
49. McCain, J.D. “Evaluations of Novel Particulate Control Devices,” EPA-600/7-78-093 [NTIS PB-283 973], Environmental Protection Agency Industrial Environmental Research Laboratory: Research Triangle Park, NC, June 1978.
50. Blythe, G., Galloway, C., and Rhudy, R.G. “Flue Gas Sulfuric Acid Measurement Method Improvements,” Proceedings of the AWMA EPRI-DOE-EPA Combined Utility Air Pollution Control Symposium, Session 18, Paper 202: Chicago, IL, August 2001.
51. U.S. Environmental Protection Agency. Method 8: 40 CFR Part 60, Appendix A. U.S. Code of Federal Regulations.
52. Cheney, J., and Homolya, J. “Characterization of Combustion Source Sulfate Emissions with a Selective Condensation Sampling System,” EPA 600/9-78-020a [NTIS PB287-436], Environmental Protection Agency Industrial Environmental Research Laboratory: Research Triangle Park, NC, 1978.
53. Maddalone, R., and Garner, N. “Process Measurement Procedures—H_2SO_4 Emissions,” EPA 600/7-79-156 [NTIS PB80-115959], Environmental Protection Agency Industrial Environmental Research Laboratory: Research Triangle Park, NC, July 1979.
54. Marchant, G.H., and Monroe, L.S. “Stack Emissions Evaluations and Characterization Tests,” Southern Research Institute, Birmingham, AL, SIR-ENV-96-126-8786.1F, February 1996.
55. Winberry , Jr., W.T. “Technical Assistance Document for Monitoring Sulfuric Acid Vapor from Stationary Sources” EPA-600/4-85-005 [NTIS PB85-143261], Environmental Protection Agency Environmental Monitoring Systems Laboratory:

Research Triangle Park, NC, January 1985.

56. Sonnenfroh, D.M.,, Wetjen, E.W., Miller, M.F., Allen, M.G., Gmachl, C., Capasso, F., Hutchinson, A.L., Sivco, D.L., Baillargeon, J.N., and Cho, A.Y. "Mid-IR Gas Sensors Based on Quasi-CW, Room-Temperature Quantum Cascade Lasers," AIAA 2000-0641, Proceedings, 38th AIAA Aerospace Sciences Meeting & Exhibit: Reno, NV, January 2000.
57. Farthing, W.E. "Development of a Low Maintenance, Field Ruggedized SO_3 CEM," US DOE Cooperative Agreement DE-FC26-02NT41593, October 2002.
58. Jackson, J., Hilton, D.A., and Buddery, J.H. "Continuous Measurement of Sulphuric Acid Vapour in Combustion Gases Using a Portable Automatic Monitor," *J. Inst Energy*, 54: 124-135, September 1981.
59. Dickson, W. "Comparison of Automated and Manual Sulfuric Acid Sampling Systems," Southern Research Institute Final Report, EPA Contract No. 68-02-3461, January 1982.
60. Blythe, G., McMillan, R., Davis, J., Lamison, M., Rhudy, R.G., Beeghly, J., Benson, L., and Goetz., E. "Furnace Injection of Alkaline Sorbents for Sulfuric Acid Control," Proceedings, AWMA EPRI-DOE-EPA Combined Utility Air Pollution Control Symposium, Session 18, Paper 201: Chicago, IL, August 2001.
61. Altman, R., Buckley, W., and Ray, I. "Wet Electrostatic Precipitation Demonstrating Multiple Pollutant Control in Industrial Applications Holds Promise for Coal-Fired Utility Emission Reduction of Acid Mist, PM2.5 and Mercury," Proceedings, AWMA EPRI-DOE-EPA Combined Utility Air Pollution Control Symposium, Session 13, Paper 205: Chicago, IL, August 2001.
62. Felix, L.G., Gooch, J.P., and Heaphy, R.F. "An Electrifying New Solution to an Old Problem," *Pollut. Eng*., July 2000, pp. 38-42.
63. Harrison, W.A., Easom, B.H., Smolensky, L.A., Wysk, S.R., Altman, R.F., and Hardman, R.R. "Pilot Scale Demonstration of a Compact Hybrid Particulate Collector (COHPAC) for Control of Trace Emissions and Fine Particles From Coal-Fired Power Plants," Proceedings, 22nd International Conference on Coal Utilization and Fuel Systems: Clearwater, FL, March 1997.
64. Heaphy, R., Cushing, K.M., and Gooch, J.P. "Improved Control of Primary Fine Particulate Emissions with Electrostatically Augmented Fabric Filtration," Proceedings, Combined Power Plant Air Pollutant Control Mega Symposium, Session 11, Paper 151: Washington, DC, May 2003.
65. Monroe, L.S., and Cushing, K.M. "Testing of a Combined Dry and Wet Electrostatic Precipitator for Control of Fine Particulate Emissions from a Coal-Fired Boiler," Proceedings, EPRI-DOE-EPA Combined Utility Air Pollutant Symposium:

Washington, DC, August 1997.
66. Cushing, K.M., Felix, L.G., and Merritt, R.L. “Field Tests of Fabric Filters on Full-Scale Coal-Fired Utility Boilers, Volume 2,” SRI-88-366, Southern Research Institute: Birmingham, AL, April 1988.
67. Gooch, J.P., and Marchant, G.H. “Electrostatic Precipitator Rapping Reentrainment and Computer Model Studies,” FP-792, Vol. 3, Electric Power Research Institute: Palo Alto, CA, August 1978.
68.